Molecular dynamics method in statistical physics

A. N. Lagar'kov and V. M. Sergeev

Institute of High Temperatures, Academy of Sciences of the USSR, Moscow
Usp. Fiz. Nauk **125**, 409–448 (July 1978)

An analysis is made of the results obtained in investigations of dense media by the molecular dynamics method. This method is based on mathematical simulation of the motion of a sufficiently large number of particles with a given interparticle interaction law. The attention is concentrated on new physical ideas about the nature of simple liquids and dense gases which have made their first appearance, have been derived, or confirmed in studies carried out by the molecular dynamics method. The principal laws of particle motion and their influence on the form of the temporal velocity correlation function are considered. Spatial and temporal correlations appearing in dense systems are studied and their role in the propagation of longitudinal and shear waves is discussed. An analysis is made of the results of molecular dynamics investigations of thermodynamic and transport properties of simple liquids and dense gases. The dynamics of a light classical particle in a dense medium of disordered heavy scatterers is discussed. Consideration is given to the close relationship between the behavior of the temporal velocity correlation function of a particle, its spatial velocity correlation function, and "percolation" in a random field of heavy scatterers.

PACS numbers: 34.10. + x, 05.60. + w, 05.70. – a, 46.10. + z

CONTENTS

INTRODUCTION

Liquids, melts, dense plasmas, and some other dense systems without an ordered structure are characterized by a property which causes serious difficulties in the development of the theories of their properties: the average kinetic energy per particle, E, is of the order of the potential energy U. The absence of a small parameter in terms of which expansions can be made is responsible for the lack of rigorous theories of liquids and melts of the same kinds that are available, for example, for solids ($E/U \ll 1$) or gases ($E/U \gg 1$).

In spite of the fact that considerable progress has been made recently in studies of dense disordered systems, which is particularly true of the physics of simple liquids,[1,3] theoretical investigations of such systems are still far from the precision attainable experimentally. Moreover, many qualitative results obtained in the physics of simple liquids are usually based on the data deduced by the molecular dynamics (MD) method. This is a basically new method for investigating strongly interacting systems of many particles; this method owes its origin to rapid progress in computational techniques. It is based on mathematical simulation of the motion of a sufficiently large number of particles with a given interaction law. Numerical solutions of the equations of motion are used to find dynamic trajectories of particles and then the ergodic hypothesis is applied to determine the Gibbs averages of any dynamic variables.

The MD method was first put forward by Alder and Wainwright[2] for investigating the motion of a system of hard spheres. Over the years, this method has been developed greatly and it is currently applied extensively in studies of thermodynamic and transport properties of dense systems. It successfully supplements the Monte Carlo method in investigations of thermodynamic properties[5] and is so far the only numerical method for studies of the dynamics of dense media.

The following variant of the MD method is now used universally. A classical system of several tens or hundreds of particles with a given interaction potential is considered. The classical equations of motion of these particles are solved numerically by different

 0038-5670/78/070566-23$01.10

methods, for example,[14]

$$\left.\begin{aligned} p_i^{k+1} &= p_i^k + \Delta t \sum_j F_{ij}(x^k), \\ x_i^{k+1} &= x_i^k + \frac{\Delta t p_i^{k+1}}{m_i}, \end{aligned}\right\} \tag{I.1}$$

where p_i^k is the momentum of the i-th particle at the k-th step; x_i^k is the coordinate of the i-th particle at the k-th step; m_i is the mass of the i-th particle; F_{ij} is the force exerted on the i-th particle by the j-th particle. For simplicity, the above formulas are given for a one-dimensional system. In solving the equations of motion it is usual to impose periodic boundary conditions in the following way. A periodic lattice with a unit cubic cell V filled with N particles (Fig. 1) is assumed. If any one particle crosses the face of a cube and carries a momentum $\mathbf{p}_i$, another particle with the same momentum enters through the opposite face symmetrically relative to the plane passing through the center of the cube. In the calculation of the forces acting on a particle, the latter is surrounded by a cubic volume V' and only the interaction with particles inside this volume V' is considered. (The relevant volume V' for particle 4 is shaded in Fig. 1.) The exceptions to this rule are systems with the long-range Coulomb interaction potential, when sometimes it is necessary to use the Ewald method in calculating the interaction energy.[135]

The particle trajectories $\mathbf{p}_i(t)$ and $\mathbf{r}_i(t)$ found in this way can be used to derive information on the thermodynamic and kinetic properties of a many-particle system by temporal averaging of the appropriate functions of dynamic variables along a classical trajectory of the system:

$$\langle f \rangle = \lim_{T\to\infty} \frac{1}{T} \int_0^T f[\mathbf{p}(t), \mathbf{r}(t)]\, dt, \tag{I.2}$$

where $\langle \cdots \rangle$ denotes the Gibbs averages of some function of the dynamic variables $\mathbf{p}$ and $\mathbf{r}$. It is assumed that the investigated system is ergodic.

In the first investigations by the MD method[2,10] considerable space was devoted to verification that the general laws governing the motion of a classical many-particle system are satisfied: these include energy conservation, establishment of a temperature defined in terms of an average kinetic energy per particle

$$\frac{3}{2} kT = \overline{E} = \left\langle \frac{1}{N} \sum_{i=1}^{N} \sum_{\alpha=1}^{3} \frac{m (v_i^\alpha)^2}{2} \right\rangle, \tag{I.3}$$

and relaxation to the Maxwellian particle velocity distribution. It was shown there that an equilibrium temperature and Maxwellian distribution are established in a time of the order of a few collision times. As expected, this is true of a very great variety of systems and is practically unaffected by the nature of the interaction potential. The problems tackled by the MD method have become gradually more complex. At present the MD method provides substantial help in understanding the structure of liquids and gases and in seeing, in the literal sense, and analyzing the complex dynamic picture of the motion of particles in a dense medium. In recent years the use of powerful computers has made it possible to employ extremely complex models with spherically asymmetric potentials of the interaction between particles. Only a few years ago it had seemed that such models were inaccessible for investigation. At present, the results obtained by the MD method are often regarded as no less reliable than the experimental data, and they are stimulating further progress in developing theories of dense gases and liquids.

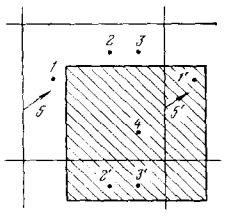

FIG. 1. Periodic boundary conditions. Particle 5′ leaves the volume V and particle 5 enters this volume.

The present review is devoted mainly to the new physical ideas first obtained, or unambiguously confirmed, by the MD method. In view of this, we shall be unable to give sufficient attention to the enormous numerical material obtained by the MD method and clearly of intrinsic interest in practical applications. The reader interested in these topics is directed to the references which will be made to these results later.

1. MOTION OF PARTICLES IN LIQUIDS AND DENSE GASES

a) Verification of models of particle motion by the molecular dynamics method. Temporal velocity autocorrelation function

Naturally, the first MD investigations were devoted to simple models, namely to systems composed of hard spheres (in the three-dimensional case) or disks of identical radius (in the two-dimensional case). At temperatures and densities higher than certain critical values, such model systems describe satisfactorily the behavior of real dense gases composed of spherical molecules. At high temperatures and for moderate densities the attractive part of the potential can be regarded as a weak perturbation. These assumptions, dating back to van der Waals, have inspired a careful study of the main laws governing the behavior of systems of hard spheres and disks, carried out by the group led by Alder.

One of the basic ideas on the nature of transport processes in liquids and dense systems is the hopping diffusion mechanism.[11] According to this concept, a molecular flux is transferred by jumps of length of the same order as the intermolecular distance. These jumps occur rarely: they take place only when neighbors usually surrounding a molecule become sufficiently widely separated to permit a jump past them. This diffusion mechanism is analogous to that employed in the theory of vacancies. Clearly, in this case there should be two characteristic mean free paths: one corresponding to "beats" of a particle in its cell and the other of the order of the intermolecular distance.

If we introduce the probability $\mathscr{P}(r)dr$ that a molecule travels from r to $r+dr$ between successive collisions, it follows that in the hopping mechanism we may expect a distribution $\mathscr{P}(r)$ with two peaks. However, calculations carried out by the MD system for a system of hard spheres have demonstrated[12,13] that the distribution $\mathscr{P}(r)$ decreases monotonically. Figure 2 shows the dependence of $\lambda\mathscr{P}(r)$ on r/λ, where $\lambda = [\sqrt{2}\,\pi n\sigma^2 g(\sigma)]^{-1}$ is the mean free path, defined in accordance with Enskog[14] that allows for the higher probability of collisions in denser systems; σ is the diameter of a hard sphere; $g(\sigma)$ is the radial distribution function for two spheres in contact. We can see from Fig. 2 that the distribution of mean free paths in a hard-sphere liquid (with the scale introduced above) is practically independent of the density and agrees (apart from a few percent) with the exponential distribution for an ideal gas. This distribution demonstrates convincingly that a molecular flux in a system consists of a large number of small jumps rather than a few large ones. A comparison of the results obtained for densities corresponding to that in a solid demonstrates similarity between the transport mechanisms considered here and those in a solid, except that the distribution curve for a solid lies lower than for a liquid, especially at high values of r. It follows that even in a solid the hopping mechanism of diffusion does not occur. In spite of the presence of vacancies, diffusion in a solid is due to a large number of small jumps which have a much higher probability than jumps of the order of the intermolecular distance.[13]

One of the most sensitive indicators of the average characteristics of the motion of particles is the temporal velocity correlation function (TVCF). Investigations of this function by the MD method have made it possible to answer a number of questions essential for the understanding of the principal laws governing the motion of particles in liquid and dense matter: 1) how important is the role of spatial and temporal correlations in the motion of particles and what are the correlation-induced deviations from the representations based on the use of stochastic-type transport equations; 2) how collective motions are established in a system of this kind.

Figure 3 shows the TVCF of a system of hard spheres obtained for various densities.[15,16] For comparison, this figure includes the exponential dependence expected on the basis of the Enskog theory.[14] The TVCF demonstrates the occurrence of collective motion of two types. In the range of moderate-density gases, the TVCF has a long positive tail extending to times of the order of 20 collision times.[16] The other type of collective motion is observed near the solidification line, for example, near the triple point, where the TVCF becomes negative after one or two collisions and remains negative for several relaxation times.[12,15]

At moderate densities a moving particle drags the particles surrounding it along with itself in the direction of the initial motion. These particles being dragged dragged aid in maintaining the velocity of the particle under consideration, tending to push it along in the original direction after a suitably long time. Collective motion of this type was first predicted by Alder and Wainwright for a system of hard spheres[16] and confirmed by them later by more detailed investigations.[17] Alder and Wainwright[17] found that the decay of the TVCF of a system of hard spheres obeys the $t^{-3/2}$ law after a suitably long time, whereas in the case of a two-dimensional system of hard disks the TVCF falls in accordance with the t^{-1} law. The motion of particles responsible for such a very slow fall is collective and it involves so many particles that we can use the laws of hydrodynamics to describe it. The decay proportional to $t^{-3/2}$ can indeed be explained by the hydrodynamic motion of a drop of particles as a whole. This idea was confirmed by Alder and Wainwright[17] by numerical solution of the Navier–Stokes equation in the Eulerian and Lagrangian coordinates for an element of volume traveling in a liquid. The size of this volume is taken to be equal to the volume per molecule and the initial velocity to be the rms velocity of the molecules. A comparison of the description of the flow resulting from the MD calculations and that found by investigating a

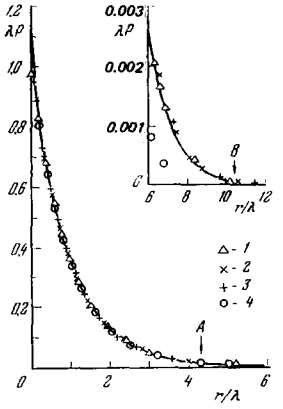

FIG. 2. Distribution of the mean free paths plotted as a function of the reduced length at various densities V/V_0: 1) 3; 2) 2; 3) 1.6; 4) 1.42. Here, V_0 is the close-packed volume. The continuous curve corresponds to infinite rarefaction. The arrows A and B identify the diameters of a hard sphere for $V/V_0 = 3$ and 2, respectively.

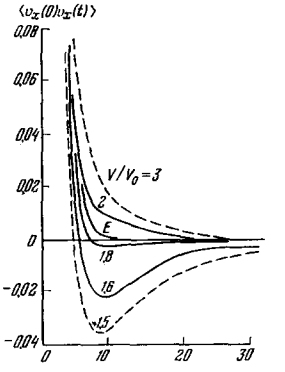

FIG. 3. Temporal velocity correlation functions of a system of hard spheres for different densities V/V_0. Curve E corresponds to the Enskog Theory. The continuous curves are calculated for 108 particles and the dashed ones for 500. The abscissa gives time expressed in units of the average interval between collisions.

hydrodynamic flow field has established good agreement between the values of the TVCF calculated for long times.

It should be stressed that the above hydrodynamic model differs basically from the Stokes–Einstein model in which a sphere representing a molecule moves slowly and adiabatically in a viscous liquid and the retardation force is assumed to have a quasistationary value, proportional to the velocity, at every moment. As a result, the velocity is found to decrease exponentially. In contrast, Adler and Wainwright[17] found the exact time-dependent solution of the Navier–Stokes equation. The hydrodynamic approach to flow demonstrated the presence of a double vortex in the two-dimensional case and of a vortex fing in the three-dimensional situation. These results showed how a positive velocity correlation results from the collective motion of particles which tend to maintain the original direction of motion of a given particle over a long time.

A large cell is needed to attain the asymptotic regime after a long time. One then faces two conflicting requirements: on the one hand, it is necessary to consider a time sufficiently long to ensure that the system can be described by the hydrodynamic equations; on the other, the time t should not be so long that an acoustic wave resulting from the periodic boundary conditions traverses the system, i.e., $t < L/v_{ac}$, where L is the edge of the cell. If a rigorous approach is made from this point of view, then the three-dimensional system ($N = 500$) used by Alder and Wainwright[17] is far too small to establish accurately the asymptotic $t^{-3/2}$ law. In the two-dimensional case, it is clear that hydrodynamic equations can be used.[18] However, an investigation[19] of a system with 4000 particles interacting in accordance with the repulsive part of the Lennard-Jones potential has confirmed the validity of the asymptotic decay $t^{-3/2}$ law established earlier.[16,17] Several theoretical studies[18,20-23] of the asymptotic behavior of the TVCF have shown that

$$\langle v(0)\, v(t)\rangle \xrightarrow[t\to\infty]{} \frac{(2kT}{\rho m}\,[4\pi(D+\nu)\,t]^{-3/2}, \qquad (1.1)$$

where ν is the kinematic viscosity; D is the diffusion coefficient; ρ is the density.

It seems to us that the most consistent approach to the asymptotic behavior of the TVCF was put forward by Fisher.[23] According to Fisher,[23] a particle drifts in the company of its neighbors and, since it travels together with the surrounding element of volume, the diffusion coefficient in Eq. (1.1) should be the Lagrangian quantity D, describing the diffusion of a drop of characteristic size $R = (8/3)\sqrt{\tau\nu}$, where τ is the relaxation time of the viscous stresses. This Lagrangian diffusion coefficient is considerably smaller than the microscopic diffusion coefficient.

It should be pointed out that the idea that a selected diffusing atom is strongly coupled to its neighbors and, therefore, its diffusion should be regarded as a collective process was proposed earlier by Frenkel.[131] Later, Egelstaff[132] based his analysis on the picture of diffusion as a collective phenomenon assuming that certain groups of atoms bound tightly to one another (globules) participate in the Brownian motion. However, the question of the relationship between the decay of the drift velocity after a long time and the rate of decay of hydrodynamic fluctuations was first formulated correctly and solved by Fisher.[23] He found that the attainment of the hydrodynamic regime by a particle may precede the execution on the average of even one jump. This picture of molecular motion shows that the numerous earlier investigations in which the motion of a particle in a liquid is divided into two parts, vibrational collective motion corresponding to short times and single-particle diffusion, have given an incorrect description of the motion of particles in a liquid. A Fourier analysis of the velocity correlation function[10] by the MD method and the results of inelastic noncoherent neutron scattering[133] demonstrate that vibrational modes are strongly damped and the transition from short times to times corresponding to diffusion occurs very smoothly after a long time with the diffusion process in a liquid still having a collective nature.

As the density increases, approaching the triple point, a different type of collective motion plays an increasingly important role and it gives rise to a negative part of the TVCF (see curve $V/V_0 = 1.5$ in Fig. 3). As at lower densities, a particle drags its environment. In the case of very high densities a particle on the average reverses its trajectory because of a barrier formed by the surrounding hard spheres. This gives rise to a negative part of the TVCF. After a time, the trajectories of the surrounding particles are also reversed and this begins to maintain the reversed motion. Consequently, the TVCF acquires an extended negative plateau stretching to times of the order of the relaxation time. Clearly, the role of the negative temporal correlations increases as the density increases and this results in the disappearance of the diffusion coefficient in the crystalline state.

A careful study of the hard spheres model has improved our understanding of the structure and kinetics of dense media. However, this model does not provide an adequate description of the liquid state because the attractive forces are ignored completely. We may expect that in those transport phenomena in which not only the kinetic but also the potential terms are important (for example, viscosity and heat conduction), this neglect of the attractive forces at low temperatures will give considerable deviations of the predictions based on the model from the true situation.

Most probably the best description of the nature of simple liquids and dense gases is provided by a model in which particles interact with one another in accordance with the Lennard-Jones potential:

$$u(r) = 4\varepsilon\left[\left(\frac{\sigma}{r}\right)^{12} - \left(\frac{\sigma}{r}\right)^{6}\right]. \qquad (1.2)$$

If we forget, for the moment, the range of high pressures where we can expect a strong influence of the nonadditive interaction on the properties of matter, a study of this model by the MD method makes it pos-

sible to describe many features of the behavior exhibited by simple liquids and dense gases discovered by direct experiments. Hence, we may hope that the results of the MD method, so far not confirmed by experiments, describe adequately the phenomena which occur in liquid and dense states.

What are the effects of allowance for the attraction between particles? An investigation of a two-dimensional system of particles interacting with one another in accordance with Eq. (1.2) has shown[24] that the attraction between particles produces vacancies and clusters in the liquid phase. The vacancies are distributed completely at random and their sizes of the order of a few σ^2. The attraction between particles close to the edge of a vacancy creates a microscopic surface tension, which effectively prevents the particles near the edge from moving to unoccupied regions. The lifetime of these vacancies at densities encountered in liquids is 3×10^{-12} sec. Figure 4 shows the instantaneous positions of particles obtained for various values of the density and temperature. We can clearly see the cluster-like groups even at a temperature exceeding the critical value. The short-range order in the distribution of particles in a cluster explains the characteristics of the absorption spectrum of mercury dissolved in liquid argon.[24,25] Studies of the trajectories of particles carried out by Fehder[24] once more contradicted the "hopping" mechanism of diffusion in liquids and demonstrated that migrating particles are basically associated with a group all of whose members diffuse approximately in the same direction. After a long time and at high densities the nature of diffusion changes from the cluster to the chain mechanism. Figure 5, taken from Fehder's paper,[24] demonstrates these two types of collective motion. In general, the direction of motion of particles during short times is correlated with the instantaneous deviation from the symmetry of their local environment.[41] Thus, the asymmetry in the spatial distribution of neighbors determines the preferential direction of their subsequent thermal motion. A correlation of this type decays in a time of the order of 0.5×10^{-12} sec. At first sight, this microdiffusion mechanism does not agree with Fig. 5 showing an almost continuous diffusive migration at $t = 2 \times 10^{-12}$ sec. However, the point is that the thermal motion of neighbors around a diffusing particle is such as to maintain continuous or approximately continuous deviation from symmetry along the direction of motion of the particle. Thus, a particle experiences microdiffusive displacements in a local environment which itself is migrating by diffusion. This picture of the diffusion process confirms the main assumptions adopted by Fisher.[23] It is also clear why the Lagrange formulation of the diffusion processes[23] is the most suitable one for the description of the asymptotic behavior of the TVCF.

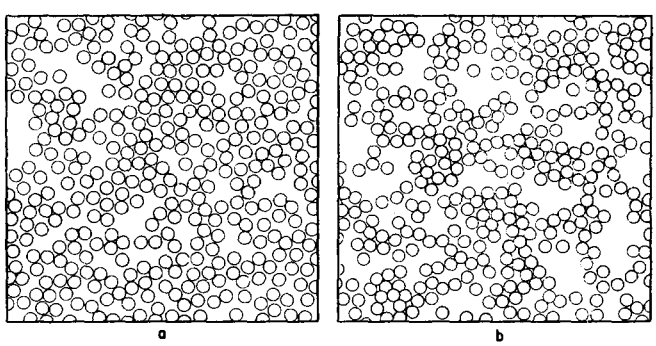

FIG. 4. Positions of particles at a certain moment: a) $T/\varepsilon = 0.927$, $\rho_R = S_0/S = 0.6781$ (S is the area of the system and S_0 is the area of a close-packed system); b) $T/\varepsilon = 1.145$, $\rho_R = 0.4645$.

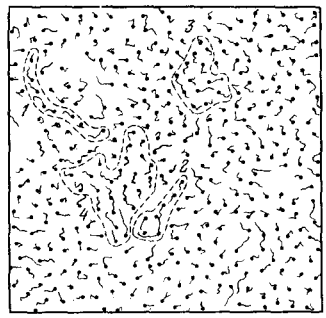

FIG. 5. Trajectories of particles during an interval of 2×10^{-12} sec ($T/\varepsilon = 0.927$, $\rho_R = 0.6781$). Small dark dots represent the centers of the particles. Lines extending from these centers are the particle trajectories. Dashed lines surround regions with diffusive migration of different kinds. Regions 1 and 2 correspond to chain migration; region 2 to migration along a vacancy edge; region 3 corresponds to cluster diffusion along the direction of a vacancy; region 4 shows both types of diffusion.

The attraction between particles has the result that the duration of collisions becomes of the same order of magnitude as the time interval between collisions. A comparison of the TVCF for hard spheres[15] and for particles interacting accordance with the Lennard-Jones potential,[27] shown in Figs. 3 and 6, respectively, demonstrates that the duration of collisions has a strong influence on the form of the TVCF at short times. In the case of real liquids (and we are assuming that the Lennard-Jones potential describes well the properties of these liquids) the TVCF corresponding to small values of t is Gaussian, whereas in the case of hard spheres it is exponential. We can demonstrate that the area under the TVCF curve for a system of hard spheres is approximately 25% smaller than the corresponding area for a liquid with the Lennard-Jones

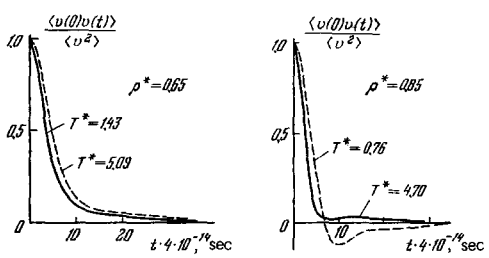

FIG. 6. Temporal velocity correlation functions of a particle in a Lennard-Jones liquid (Ar) plotted for $\rho^* = N\sigma^3/V$, $T^* = T/\varepsilon$, $\varepsilon = 119.8°K$, and $\sigma = 3.405$ Å.

potential. In this comparison the diameter of a hard sphere is selected so that, for given values of ρ and T, the height of the first structure maximum deduced by solving[28] the Percus–Yevick equation for hard spheres is identical with the corresponding height for a real liquid.

b) Autocorrelation function of forces in liquids and dense gases

An alternative (in a sense) to the hard-sphere model described in detail above is the model of the liquid state proposed by Rice and Allnatt.[30,31] This model is of of interest because of the results obtained with its aid and also because of the underlying assumptions. In the Rice–Allnatt model a liquid is regarded as a system of hard spheres which follow, in the intervals between collisions, Brownian trajectories because of interaction with the weak attractive part of the potential. Collisions due to this soft attractive part of the potential disturb the temporal correlation in the motion of these hard spheres, which can then be regarded as totally uncorrelated. These assumptions make it possible to write down the transport equations for the distribution functions. In a series of subsequent papers[32-34] it is shown how to solve these equations and determine the transport coefficients of a liquid.

One might expect the Rice–Allnatt model to describe well the behavior of liquids at low temperatures. However, the results obtained by Einwohner and Alder[13] have given rise to doubts about the validity of the Rice–Allnatt model. Einwohner and Alder[13] used the MD method to study a system with the "hard sphere + square well" interaction potential. All the collisions, apart from those between hard spheres, are regarded as "soft" and the ratio of the number of these soft collisions to the number of collisions of the hard spheres is calculated. This ratio is found to be close to 0.5. Since each soft collision has little effect on the momentum of a particle, it is not easy to see how such rare soft collisions can result in considerable weakening of temporal correlations in the motion of hard spheres.

An important component of the Rice–Allnatt theory is the formalism of the friction constant developed by Kirkwood.[136] The validity of this formalism in the Rice–Allnatt theory can be checked by investigating directly the autocorrelation function of the force acting on a particle in a liquid.

We shall now consider the formalism of the friction constant. In the Rice-Allnatt theory it is assumed that a change in the momentum of a particle between the hard-sphere collisions is described by the Langevin equation

$$\frac{dp}{dt} = -\frac{\xi}{m} p + X(t), \tag{1.3}$$

where ξ is the friction constant; $X(t)$ is a random force; $\langle X(t)\rangle = 0$; $\langle X(t)X(t+\tau)\rangle = \xi(\tau)$; $\xi(\tau)$ is the autocorrelation function of the random forces. It is assumed that $\xi(\tau) = 0$ for $\tau > \tau_1$, where τ_1 is much less than the velocity correlation time. The expression for ξ in terms of $\xi(\tau)$ can be written in the form[36,37]

$$\xi = \frac{1}{kT}\int_0^\infty d\tau \xi(\tau). \tag{1.4}$$

A very important feature of the derivation of Eq. (1.4) is the assumption about the nature of the function $\xi(\tau)$, which should have a sharp peak near $\tau = 0$ and, moreover, it is assumed that $\tau_1 \ll m/\xi$.

In this case the friction constant can also be found from the autocorrelation function of the total force F using the relationship

$$\xi = \frac{1}{3kT}\int_0^{\tau_1} \langle F(t) F(t+\tau)\rangle d\tau, \tag{1.5}$$

where τ_1 is found from the condition

$$\langle F(t) F(t+\tau_1)\rangle = 0. \tag{1.6}$$

However, the values of ξ are well defined only if the integral of (1.5) considered as a function of its upper limit varies slowly when τ changes from τ_1 to m/ξ. (We recall that $\int_0^\infty \langle F(t)F(t+\tau)\rangle d\tau = 0$.) These conditions are one of the criteria of the validity of the Rice–Allnatt theory.

Figure 7 shows the autocorrelation functions of the forces found by the MD method.[35] A deep negative minimum of the force autocorrelation function is evidence of considerable temporal correlations in the system. Clearly, the appearance of the force autocorrelation function excludes the possibility of a plateau of the integral (1.5) considered as a function of the upper limit. Moreover, the correlation time deduced from Eq. (1.6) is only one-quarter of the value of m/ξ calculated from Eq. (1.5). One should also note an additional point. The collision operators can be separated in the way it is done in the Rice–Allnatt theory only if the spectra of their eigenfunctions do not overlap. Clearly, this is true if the relaxation time of a system of hard spheres is very different from the relaxation time of a system of particles interacting in accordance with the van der Waals potential. A direct check by the MD method shows that this condition is not satisfied. A similar situation also applies to the autocorrelation function of the forces acting on a particle in a salt melt.[38] The potential of the interaction between particles in the melt can be modeled

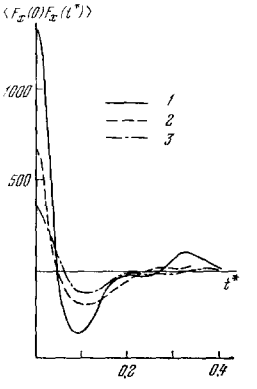

FIG. 7. Temporal correlation functions of the forces acting on a particle in a Lennard-Jones liquid (Ar), plotted for $\varepsilon = 119.8$°K, $\sigma = 3.405$ Å, $\rho^* = 0.68$, and various values of T^*: 1) 3.55; 2) 2.14; 3) 1.31.

by short-range repulsion at short distances and Coulomb interaction at longer distances. It would seem that under these conditions the application of the Rice–Allnatt model would be most acceptable.[39,40] However, a study of the force autocorrelation function of the salt melt model by the MD method[38] yields results which give rise to the same objections against the Rice–Allnatt theory as in the case of simple liquids. A similar conclusion is also reached by Smedley and Woodcock[42] on the basis of an investigation carried out by the MD method. Recent calculations of the transport coefficients[43] of liquid argon have shown that the Rice–Allnatt theory gives results that differ from the experimental values by a factor of 1.5–2. It is clear from the above discussion that the reason for this lies in the violation of the fundamental assumptions of this theory.

c) Decay of density correlations. Longitudinal and shear waves in liquids

In investigations of the microscopic properties of the liquid state it is important to consider the equilibrium density–density correlation function

$$G(r, t)=V\left\langle\sum_{i, j}^{N}\rho_i(r, t)\,\rho_j(0, 0)\right\rangle, \tag{1.7}$$

where $\rho_i(\mathbf{r}, t)=\delta[\mathbf{r}-\mathbf{r}_i(t)]$. The function G can be represented by the sum of two functions

$$G(r,t)=G_s(r,t)+G_d(r,t), \tag{1.8}$$

where

$$G_s(r,t)=V\langle\rho_i(\mathbf{r},t)\,\rho_i(0,0)\rangle. \tag{1.9}$$

The functions $G(r, t)$ and $G_s(r, t)$ were first introduced by Van Hove[44,45] in the neutron scattering theory. The function $G_s(r, t)$ gives the density of the probability of finding a particle at a point r at a moment t if at $t=0$ this particle is located at the coordinate origin. The quantity $G_s(r, t)$ can be deduced by the MD method with the aid of the expression

$$G_s(r, t)=\frac{1}{4\pi r^2\Delta r}\langle\theta(\mathbf{r}_i(t)-\mathbf{r}_i(0)-\mathbf{r})\rangle, \tag{1.10}$$

where $\theta(\mathbf{x}-\mathbf{r})=1$ if $\mathbf{x}$ lies between r and $r+\Delta r$, and it vanishes in any other case.

The function $G_d(r, t)$ is the temporal pair correlation function. It is defined as follows: if at a moment t there are $n(r, t)$ particles at a distance between r and $r+\Delta r$ from the position occupied by an atom at $t=0$, then

$$G_d(r, t)=\frac{V}{N}\frac{n(r, t)}{4\pi r^2\Delta r}. \tag{1.11}$$

The particle originally located at the coordinate origin is excluded from the calculations.

It is known[44,45] that the Fourier transform of the function $G_s(r, t)$, usually denoted by $S_s(k, \omega)$, is the differential cross section of noncoherent neutron scattering, and that the Fourier transform of the function $G(r, t)$, is the dynamic structure factor $S(k, \omega)$, which is is the differential cross section of coherent scattering. In this case $\hbar\omega$ represents the energy transferred to the system and $\hbar k$ is the modulus of the transferred momentum. Thus, the quantities $G_s(r, t)$ and $G(r, t)$ can be measured directly. However, such measurements are very time-consuming and, moreover, they do not give the dependence over the whole range of k and ω. Therefore, the MD method is extremely useful in the interpretation and prediction of the spectra of scattered neutrons. It is possible to establish how far in the short-wavelength range is the collective motion of particles still clearly observable and how collective migration changes to individual motion at very short wavelengths. It should be pointed out that the range of very long wavelengths, corresponding to the hydrodynamic regime is still beyond the reach of the MD method (as demonstrated below) but in this case information on the nature of the function $S(k, \omega)$ can be obtained from the scattering of light in liquids (Brillouin scattering). Thus, sufficiently comprehensive information is now available on the form of the function $S(k, \omega)$ for almost all the values of k and ω.

Theoretical investigations of the functions $G_s(r, t)$ and $G_d(r, t)$ have been reported in a large number of papers. The most natural and frequently employed assumption about the nature of the function $G_s(r, t)$ is that it is Gaussian. The MD method allows us to determine the true form of the function and the limits of validity of the Gaussian approximation. If $G_s(r, t)$ is Gaussian, i.e.,

$$G_s(r, t)=[4\pi A(t)]^{-3/2}e^{-r^2/4A(t)}, \tag{1.12}$$

where $A(t)=\frac{1}{6}\langle r^2\rangle$, then

$$\langle r^{2n}\rangle=C_n\langle r^2\rangle^n,$$

where $C_n=(2n+1)!!/3^n$ for $n=1, 2, 3, \ldots$.

Calculations carried out by the MD method show that the function $G_s(r, t)$ deviates from the Gaussian form.[10] The magnitude of the deviation, expressed as a function of

$$\alpha_n(t)=\frac{\langle r^{2n}\rangle}{C_n\langle r^2\rangle^n}-1,$$

is shown in Fig. 8.

Since all the values of α are positive, it is clear that an increase in r results in the approach of the true $G_s(r, t)$ function to zero at a rate slower than in the Gaussian case. In the limit $t\to\infty$ the function becomes, as expected, entirely Gaussian. This occurs in practice in a time of the order of 10^{-11} sec. The quantity $\sqrt{\langle r^2\rangle}$ is then approximately equal to the distance from the nearest neighboring particle.

For any fixed value of k the function $S_s(k, \omega)$ has a maximum at $\omega=0$ and falls off smoothly as ω increases.

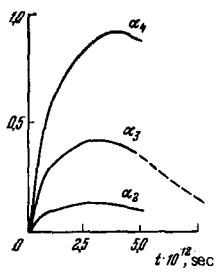

FIG. 8. Deviation of the Van Hove autocorrelation function of argon from the Gaussian form ($\rho=1.374$ g/cm^3, $T=94.4$°K).

The half-width $\omega_{1/2}$ at midamplitude of $S_s(k, \omega)$ and the value of $S_s(k, 0)$ can be used to determine the deviation of $S_s(k, \omega)$ from a dispersion curve typical of the long- and short-wavelength limits. Figure 9 shows the behavior of the quantities $\Sigma(k) = \pi k^2 D S_s(k, 0)$ and $\Delta(k) = \omega_{1/2}/k^2 D$, as a function of k. In the hydrodynamic limit, these quantities tend to unity. The half-width has a minimum near $k \sim 2\text{Å}^{-1}$, which corresponds to the first maximum of the structure factor $S(k)$. This narrowing shows that the spatial correlation of particles has a considerable influence on the Van Hove autocorrelation function. This narrowing is associated with the deviation of $G_s(r, t)$ from the Gaussian form.[46] The nature of the function $\Delta(k)$ obtained by the MD method[46] and supported by later neutron scattering experiments[133] is in conflict with the predicted dependences, as pointed out by Schofield.[1] This is due to the fact that the form of the function

$$g(\omega) = \frac{m}{3\pi kT} \int_{-\infty}^{\infty} \langle v(0)\, v(t) \rangle\, e^{i\omega t}\, dt,$$

used by Schofield, does not represent the true behavior of $g(\omega)$ obtained already by the MD method.[10]

We shall now consider the results derived by the MD method using the dynamic structure factor $S(k, \omega)$ and and the associated Fourier transform of the correlation function of longitudinal currents $C_\parallel(k, \omega)$. The correlation function of these currents is defined as follows:[1]

$$C_\parallel(k, t) = k^2 \langle J_\parallel(k, 0)\, J_\parallel^*(k, t) \rangle, \tag{1.13}$$

where

$$J_\parallel(k, t) = \sum_{i=1}^{N} v_i^z(t)\, e^{ikz_i(t)}. \tag{1.14}$$

Clearly, $\mathrm{Re}\, C_\parallel(k, \omega) = \omega^2 S(k, \omega)$. The form of the function $S(k, \omega)$ obtained by the MD method near the triple point is shown as a function of ω in Fig. 10. We can see that for wave vectors smaller than $1/\sigma$ the system under consideration exhibits phonon peaks. These peaks are due to the Brillouin scattering; their maxima correspond to the values of ω/k equal approximately to the macroscopic velocity of sound. It should be pointed out that the use of the hydrodynamic theory with just one relaxation time of viscous stresses fails to predict such maxima. The theoretical maxima disappear for values of k much smaller than those given by the MD calculations. However, we shall show later that the approximation for single relaxation times is invalid near the triple point. The hydrodynamic theory with two relaxation times of viscous stresses describes well the range of small values of k attainable in the MD calculations and predicts corresponding phonon peaks.[134] However, these peaks are greatly broadened and the

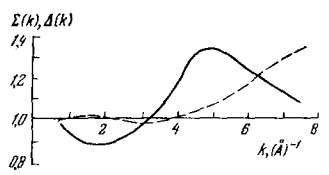

FIG. 9. Deviations of the values of $\Sigma(k)$ and $\Delta(k)$ from the hydrodynamic limit, deduced from MD calculations[50] for Ar, $\rho^* = 0.8442$, $T^* = 0.722$, $\varepsilon = 119.8°\text{K}$, and $\sigma = 3.405$ Å.

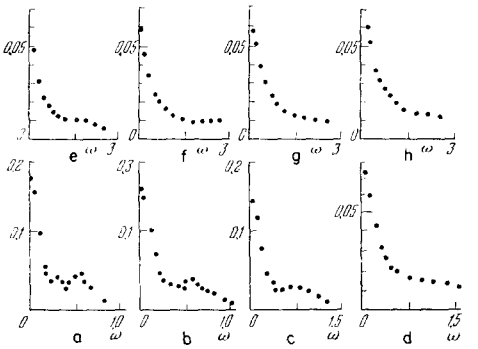

FIG. 10. Function $2S(k\omega)/\pi$ for the same model as in Fig. 9. The results of MD calculations are given for eight values of k: a) 0.623; b) 0.752; c) 0.881; d) 1.366; e) 1.931; f) 2.534; g) 3.182; h) 3.812. The values of k are given in units of σ^{-1}, and those of ω in units of τ^{-1} ($\tau_0 = \sqrt{m\sigma^2/48\varepsilon} = 3.112 \times 10^{-13}$ sec).

vibrations are damped out rapidly. In the $k > 1\ \text{Å}^{-1}$ range there is no oscillatory behavior of the density fluctuations. In this range they are strongly damped and cease to propagate. However, fluctuations of the current continue to propagate and their frequency and lifetime depend strongly on the structure factor $S(k)$. Indeed, the MD investigations of $C_\parallel(k, t)$ demonstrate oscillatory behavior of this function[49,51] over a wide range of values of k. Consequently, the function $C_\parallel(k, \omega)$ exhibits a maximum at $\omega \neq 0$. The magnitude of this maximum is plotted as a function of k in Fig. 11, which demonstrates a well defined dispersion curve. This figure also includes a plot of the average lifetime of the current fluctuations. It is quite clear that the maximum lifetime is exhibited by the largest-scale fluctuations.

The dispersion curve $\omega_{\max}(k)$, found by the MD method has two maxima.[51] The position of the second maximum agrees approximately with the position of the first minimum of $S(k)$. This demonstrates a close relationship between the propagating vibrations and the structure. Later experiments on neutron scattering[133] have confirmed the existence of the second maximum and there are now many theoretical papers in which the dispersion curve is reproduced with satisfactory accuracy over a wide range of the parameter k (see

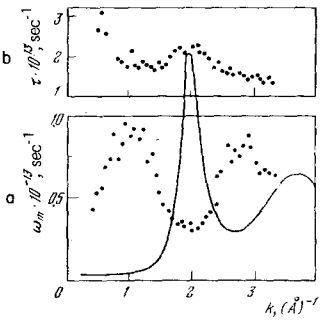

FIG. 11. Position of a maximum ω_m of the function $C_\parallel(k, \omega)$ (a) and average lifetime of longitudinal currents τ (b) plotted as a function of k for Ar, $\rho = 1.407\text{g/cm}^3$, $T = 70°\text{K}$, $\varepsilon = 119.8°\text{K}$, and $\sigma = 3.405$ Å. The dots are the results of MD calculations[51] and the continuous curve is the structure factor $S(k)$ in relative units.

Skold *et al.*[133] and the references given there).

In the range of high values of k, much greater than the reciprocal of the interatomic distance, the term $i \neq j$ in the correlation function of the currents becomes small and this function depends only on the single-frequency modes but is no longer the collective coordinate of these modes. Consequently, the function $S(k, \omega)$ becomes equal to the correlation function $S_s(k, \omega)$ and, for high values of k, it tends to the gaskinetic limit, whereas the dispersion curve $\omega_{max}(k)$ reaches at high values of k the asymptotic value $\omega_{max}(k) = k\sqrt{2k_BT/m}$.

It should be pointed out that neutron scattering experiments demonstrate similarity between scattering in liquids and in polycrystalline solids. This similarity is quite reasonable, as shown in Fig. 12, which shows the behavior of the function $G_d(r, t)$ obtained by the MD method.[10] Decay of the spatial pair correlation function $g(r)$ [we recall that $G_d(r, 0) = g(r)$] demonstrates retention—for a long time—of spatial correlations resembling the correlations in a solid. Even after $t = 2.5 \times 10^{-12}$ sec we can still clearly see a short-range cell. This circumstance justifies to some extent both the attempts to consider a liquid from a "quasicrystalline" point of view and also the introduction of the phonon concept in the theory of liquids, because we can speak of phonons only if the initial structure $G_d(r, 0)$ does not decay in the phonon lifetime. However, we must recall that at high frequencies of the density oscillations the period of these oscillations is comparable with the characteristic lifetime of the fluctuations and the phonon spectrum is practically suppressed.

All the results obtained by the MD method in investigations of the quantities $S(k, \omega)$ and $S_s(k, \omega)$ have been subsequently confirmed experimentally by neutron scattering.[133] These results have served as the basis of various approximate models for the calculation of the quantities $S(k, \omega)$ and $S_s(k, \omega)$. The interested reader can find more information on this subject in the relevant papers.[47,48]

We shall now discuss the results obtained in an investigation of transverse waves in liquids. Characteristics of the propagation of shear waves in a liquid can be understood by considering the correlation function of transverse currents, defined as

$$C_t(k, t) = k^2 \left\langle \sum_{i=1}^{N} v_i^x(t)\, e^{-ikZ_i(t)} \sum_{j=1}^{N} v_j^x(0)\, e^{ikZ_j(0)} \right\rangle. \qquad (1.15)$$

The MD investigations[50,51] demonstrate that the function $C_t(k, t)$ begins to oscillate when k exceeds a certain critical value k_c. In this range of k the quantity $\mathrm{Re}\,C_t(k, \omega)$ has a maximum, when considered as a function of ω, at $\omega \neq 0$. Figure 13 shows this maximum as a function of k. The curve is in qualitative agreement with with the dispersion law derived by Frenkel[131] on the basis of the viscoelastic theory. Under conditions sufficiently far from the solidification line, so that the approximation of a single relaxation time of viscoelastic stresses is justified, the value of k_c obtained from the viscoelastic theory of propagation of shear waves in a liquid is in approximate agreement with the value deduced by the MD method. Close to the triple point the approximation of a single relaxation time is invalid. Consequently, the critical value of k_c is somewhat less than the value found using a single relaxation time. It is clear from Fig. 13 that the presence of structure in a liquid has little effect on the nature of the dispersion curve of transverse currents and this is apparently due to the fact that fluctuations of these currents alter relatively little the interparticle distances, so that the restoring forces acting on the particles are also weak irrespective of the value of the wave vector.[51]

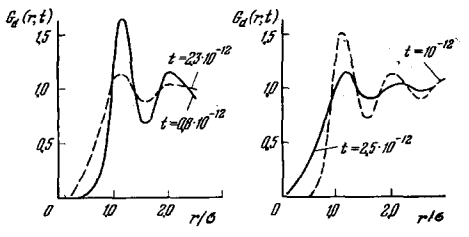

FIG. 12. Decay of the collective part of the correlation function of the density in argon ($\rho = 1.374$ g/cm^3, $T = 94.4$°K, $\varepsilon = 119.8$/k, $\sigma = 3.405$ Å).

Figure 13 includes also a plot of $\mathrm{Im}\,\omega$ found by an analysis of the MD data carried out in the approximation of a single k-dependent relaxation time.[47] A comparison of $\omega_{max}(k)$ and $\mathrm{Im}\,\omega(k)$ shows that shear waves in a liquid are strongly damped and are almost completely suppressed in one oscillation period.

We shall conclude this section by noting that the special nature of the MD method prevents us from finding the functions $C_\parallel(k, \omega)$ and $C_t(k, \omega)$ for low values of k. This is clear from an analysis of the method for calculating these quantities. Since we are considering a system with periodic boundary conditions, it follows that the only nonvanishing Fourier components are those which are characterized by $k = (2\pi/L)(m_1, m_2, m_3)$, where m is a positive or negative integer. Selecting a certain value of k and knowing the positions and velocities of N particles, we can calculate any required dynamic quantity. The dependences on $|k|$ of $C_\parallel(k, t)$ and $C_t(k, t)$ are obtained by adding the results for all the values of k lying in the shell between k and $k + \Delta k$ divided by the number of vectors k in the shell (for the selected value of Δk). Clearly, the angular averaging

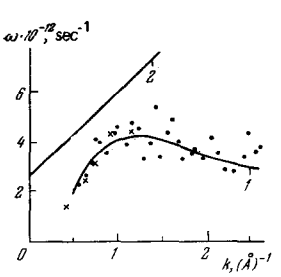

FIG. 13. Position of the maximum of Re $C_t(k, \omega)$ plotted as a function of k. The dots are the results of MD calculations[51] for the same model as in Fig. 11. The continuous curve l is found by averaging the MD results. The crosses are the results of MD calculations[50] for the same model as in Fig. 10. Curve 2 represents the damping coefficient Im ω of transverse currents under the same conditions as in Fig. 11.

of k in the range of small values of k is statistically less satisfactory than at high values of k. It is basically incorrect to consider oscillations of wavelength comparable with the dimensions of an MD cell. Therefore, the MD method is restricted to investigations of the values of k exceeding 0.2 $Å^{-1}$. It follows that the range of small values of k and ω, where the use of the hydrodynamic approximation still raises doubts, has been poorly investigated. The use of fast computers, enabling the investigator to increase the number of particles in an investigated cell, will soon make it possible to obtain reliable MD results also in this intermediate range.

2. THERMODYNAMIC PROPERTIES AND TRANSPORT PHENOMENA IN SIMPLE LIQUIDS AND DENSE GASES

a) Phase transitions

Recent investigations[52] have shown that "numerical experiments" and, in particular, the MD method can contribute greatly to the understanding of the qualitative laws in the theory of phase transitions. Even in the simplest system consisting of hard spheres the existence of a solidification (fusion) line has not been obvious and it has been doubted on many occasions. The interest in this subject has increased still further on discovery[53,54] that a physically reasonable solution of the Born–Green equation cannot be obtained at farily high densities in a hard-sphere system. This has been interpreted as indicating the occurrence of a phase transition.[1] Singularities in the solution of the Born–Green equation appear at a reduced density $\rho\sigma^3 = 0.95$ (close packing corresponds to $\rho\sigma^3 = 1.414$). However, investigations of the Percus–Yevick equation,[54] which give much better results for the equation of state than the Born–Green equation, have revealed the absence of such singularities. Thus, a sufficiently convincing proof of the existence of a phase transition in a hard-sphere system has been lacking and the question has remained open. An investigation of the system of 500 hard spheres by the MD method[55,56] has demonstrated that the nature of motion of the particles changes radically at some critical density. Near the close-packed state the particles move around certain positions of equilibrium, but on increase of the volume by 30% the system begins to "flow." Near the critical volume there is an instability of the motion in time and the system apparently changes from the liquid to the solid state and vice versa. Such behavior can be regarded as a phase transition. However, even these results are not sufficiently convincing. A three-dimensional system of 500 particles is too small to demonstrate the existence of a phase transition because the influence of the boundary conditions is too great. The coexistence of phases in such a system has not yet been proved. Therefore, an attempt has been made to demonstrate the existence of a phase transition in a hard-disk system.[57] A two-dimensional system of 870 hard disks is effectively much "larger" than a system of 500 hard spheres since the influence of the boundary conditions

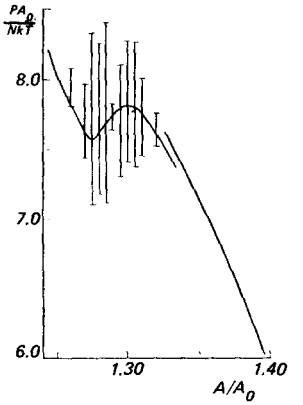

FIG. 14. Equation of state of hard disks in the region of a phase transition.[57] Here, A/A_0 is the ratio of the area of the system to the close-packed area. The vertical bars represent fluctuations of the compressibility factor found by averaging over 5×10^4 collisions; the continuous curve represents averaging over 10^7 collisions.

in the former case is less. This system was investigated over a time interval corresponding to several million collisions. It was found that the dependence of the compressibility on the density resembles very closely the van der Waals equation of state (Fig. 14). Fluctuations of the pressure near the critical density were investigated by dividing the trajectory of the system into segments of 50 000 collisions and the averaging was carried out over all those segments. The vertical marks in Fig. 14 show the dependence of the magnitude of the fluctuations on the density. A strong increase in this magnitude near the critical density demonstrated the occurrence of a phase transition. It was possible to demonstrate the existence of solid and liquid phases in the investigated system of 870 disks. Figure 15 shows clearly the coexistence of two regions of a solid and of a liquid layer between them. Thus, the MD method provides a very convincing proof of the occurrence of a phase transition in a hard-disk system. Since there is no attraction in hard-sphere and disk systems, it is clear that this phase transition is of purely geometric nature. It is most likely associated with the appearance of a shear instability in the motion of particles in a solid on increase of its volume. In fact, in a close-packed state it is not possible to shift one layer of particles relative to another but slip becomes possible when the volume of the system is increased. A comparison of systems of 72[58] and 870[57] disks clearly makes it possible to

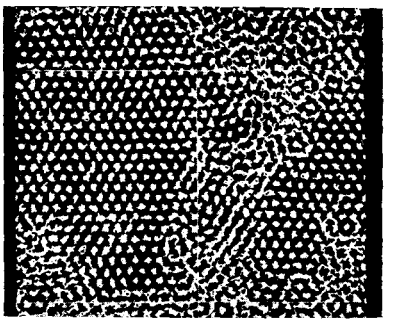

FIG. 15. Tracks of centers of particles in a system of 870 hard disks near a phase transition.

extrapolate the results obtained by the MD method for 500 hard spheres to a system with a larger number of particles. In the case of 72 hard disks the coexistence of phases is not observed but in the region of the critical density the system goes over alternatively to the solid and liquid states. This dependence of the behavior of a system on the number of particles is explained by the fact that the surface energy at a phase boundary is very considerable. Fluctuations in a small system are insufficiently strong to provide conditions for the existence of a phase boundary. The situation is different for a system of 870 disks. The free surface energy at the phase boundary, calculated per particle,[58] is only $\sim kT/60$, i.e., it is small compared with the average kinetic energy of a particle so that the existence of the phases is possible and is indeed observed. (It should be recalled that in the case of a system of hard spheres the contribution to the free energy of a phase boundary is made only by the surface entropy.) The absence of phase coexistence in a system of 72 disks does not mean that there is no phase transition. In fact, the conclusion of occurrence of a phase transition follows from the ergodic hypothesis, according to which averaging over an ensemble is equivalent to averaging over time. If we observe a system with a small number of particles for a sufficiently long time, we find that the pressure derived by averaging over all such states may give rise to a plateau in the region of critical densities. This is indeed observed for the equation of state of 72 disks (Fig. 16). However, it should be pointed out that this "plateau" lies about 10% below the corresponding plateau of a system of 870 particles.

We shall conclude this subsection by mentioning that the MD method can be used to investigate not only phase transitions but also metastable states of liquids.[148,149]

b) Thermodynamic properties of simple liquids

The MD method allows us to determine not only the general laws governing the behavior of a classical many-particle system but also to investigate quantitative characteristics of systems with realistic interaction potentials such as the equation of state, internal energy, correlation functions, etc. Verlet[59] was the first to demonstrate the capabilities of this approach and to compare the results of a calculation of the equation of state based on the Lennard-Jones potential with the experimental data for argon. Since the Lennard-Jones potential is a two-parameter quantity, all the calculations should be carried out in "reduced" units employing the parameter σ as the unit of length, ε as the unit of energy, and the molecular mass as the unit of mass. Then, any thermodynamic variable of a given substance is found by multiplying the values in terms of the reduced units by a suitable combination of ε, σ, and m. In this way the MD method makes it possible not only to determine the properties of a system from a given potential but also to find the parameters of the potential by comparison with the experimental data.

The equation of state can be described by

$$\frac{pV}{Nk_BT} = 1 - \frac{1}{3Nk_BT}\left\langle \sum_{i>j} r_{ij}\frac{\partial u}{\partial r_{ij}} \right\rangle - \frac{N}{6Vk_BT}\int_{r_0}^{\infty} r\frac{\partial u}{\partial r} g(r)\, dr, \quad (2.1)$$

where r_0 is the radius equal to half the cell edge and $g(r)$ is the pair correlation function. The last term in Eq. (2.1) allows for the contribution to the pressure at distances exceeding the cell size. It can be estimated by assuming that $g(r) = 1$ for $r > r_0$. Figure 17 compares the results of calculations of the equation of state reported by Verlet[59] with the experimental data.[60] The constants of the potential ε and σ are taken to be 119.8°K and 3.405 Å, respectively.[61] The agreement between the calculations and experiment is strikingly good. Thus, a correct selection of the potential in the MD method ensures a precision close to that attainable experimentally. The results obtained by Verlet[59] demonstrate that the Lennard-Jones potential is suitable for the calculation of the thermodynamic properties of argon of almost all densities right up to the triple point. However, we have to remember that the calculations of thermodynamic properties carried out by the integral equation method[3] and also the MD calculations of the transport properties (this point is discussed later) give results which deviate increasingly from the experimental data as the density increases. The agreement can be improved by introducing the dependence of the parameters of the potential employed on the density. This is regarded as an indication of the importance of the nonadditive many-particle interaction.[3]

The suitability of the pair potential for the calculation

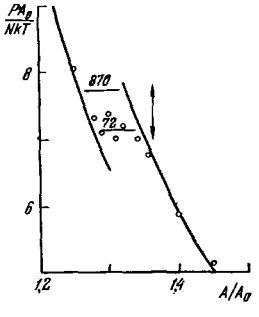

FIG. 16. Equation of state of 72 hard disks.[58] The higher horizontal line gives the compressibility factor for 870 disks.[57]

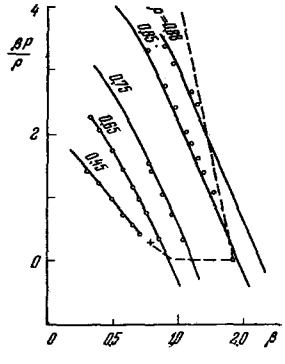

FIG. 17. Equation of state of argon. The reciprocal temperature β and the density ρ are given in reduced units, $\varepsilon = 119.8$°K, $\sigma = 3.405$ Å. The continuous curves are the results of MD calculations[59] and the circles are the experimental values.[60]

of thermodynamic properties is still a matter of controversy.[62] It is shown in several papers[62,63] that the Lennard-Jones potential for argon is not the true pair potential (which is somewhat deeper[64]) but the "effective" potential which—to some extent—allows for many-particle interactions. In fact, we can deduce the "effective" pair potential by adding a correction for the three-particle interactions to the "exact" pair potential. The result modified in this way approaches the Lennard-Jones potential.[63] The suitability of the Lennard-Jones potential in the calculation of thermodynamic properties of argon has also been demonstrated directly. A comparison of the results obtained employing the Lennard-Jones, Buckingham, and Klein–Hanley potentials,[65] in the latter of which allowance is made for attraction $\sim 1/r^8$, shows[66] that the Lennard-Jones potential is the most suitable for the calculation of thermodynamic properties.

One of the most interesting applications of the MD method is the verification of the assumptions underlying the rapidly developing theory of integral equations for the pair correlation function. This is particularly important because the results of calculations of thermodynamic properties obtained by the theory of integral equations depend on the interaction potential and a comparison with the experimental data cannot be regarded as the absolute criterion of validity. We shall consider the capabilities of the MD method by investigating the validity of the two best known integral equations for the pair correlation function: the Percus–Yevick and Born–Green equations.

The MD method makes it possible to find the pair correlation function $g(r)$ and the associated direct correlation function $C(r)$ found from the Ornstein–Zernike equation

$$h(r) = C(r) + \rho \int h(r' - r)\, C(r')\, dr', \tag{2.2}$$

where $h(r) = g(r) - 1$.

Knowing the dependences of these functions on the volume of a sample and its temperature, we can investigate the suitability of the Percus–Yevick equation

$$C(r) = g(r)\,(e^{-\beta u} - 1) \tag{2.3}$$

for the description of the structure of a liquid. A direct comparison of the pair correlation functions, calculated by the method of molecular dynamics using the Percus–Yevick equation, shows[67] that this equation gives satisfactory results only at densities below the critical value. This can be demonstrated even more clearly by calculating the compressibility factor $P/\rho kT$. For $\rho^* = 0.4$ and $T^* = 1.46$ the Percus–Yevick equation gives $P/\rho kT = 0.40$, whereas the MD method gives 0.41 ± 0.01. For $\rho^* = 0.85$ and $T^* = 0.88$, we find that the corresponding values are 3.18 and 1.64, respectively. Another way of checking the Percus–Yevick equation is to compare the intermolecular potential deduced from this equation with $g(r)$ and $C(r)$ calculated by the MD method with the Lennard–Jones potential. The results of such a comparison[67] are plotted for various densities and temperatures in Fig. 18. It follows that

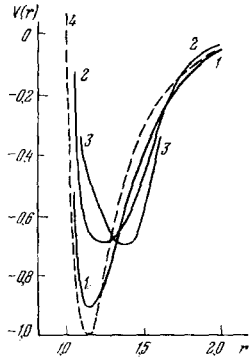

FIG. 18. Potential obtained from pair correlation functions calculated[67] by the MD method: 1) $T^* = 1.328$, $\rho^* = 0.5426$; 2) $T^* = 1.05$, $\rho^* = 0.75$; 3) $T^* = 1.127$, $\rho^* = 0.85$; 4) potentials deduced from the Percus–Yevick equation (dashed curve).

the Percus–Yevick equation is unsuitable at high values of the reduced densities and at temperatures below the critical value.

Since the MD method allows us, in principle, to obtain a correlation function of any order (two-particle, three-particle, etc.), there should be no difficulty in investigating the validity of the superposition approximation employed in the derivation of the Born–Green equation. This approximation involves the assumption that the ternary correlation function can be represented by a product of pair correlation functions

$$g(r_{12}, r_{13}, r_{23}) = g(r_{12})\, g(r_{23})\, g(r_{13}). \tag{2.4}$$

This approximation was checked by Alder,[68] who compared the function $\sqrt[3]{g_3(r, r, r)}$ calculated for a hard-sphere system and the pair correlation function. An analysis of the validity of Eq. (2.4) demonstrated that this relationship is obeyed with satisfactory precision, but the results obtained by Alder[68] cannot resolve finally the question of validity of the superposition approximation because the selected configurations are not sufficiently representative. Rahman[146] investigated a three-particle correlation function of configurations corresponding to isosceles triangles (r, r, s) in the case of a Lennard-Jones liquid. The results indicated that for s smaller than the average distance between the particles the superposition approximation overestimates the contribution of small r. Moreover, $R_r(s) = g_3(r, r, s)/[g_2(r)]^2$ has a maximum, whose position is given incorrectly in the superposition approximation.

The superposition approximation loses its validity at short distances also in the case of systems with different interparticle interaction potentials. For example, Tanaka and Fukui[147] investigated liquid sodium by the MD method retaining only the configurations corresponding to equilateral triangles (r, r, r) and to isosceles triangles (r, s, s). The results demonstrated that the superposition approximation for isosceles triangles is accurate to within 10% for r greater than the first minimum of the correlations function, but it considerably overestimates the contribution at shorter distances.

c) Transport coefficients

In the case of small deviations of a system from its thermodynamic equilibrium, the theory of linear response gives the relevant fluxes and the corresponding transport coefficients are as follows:[1]

the diffusion coefficient

$$D = \int_0^\infty \langle v_i^x(0)\, v_i^x(t)\rangle\, dt; \tag{2.5}$$

the shear viscosity

$$\eta = \frac{1}{Vk_BT}\int_0^\infty \langle \varphi_{xy}(0)\, \varphi_{xy}(t)\rangle\, dt; \tag{2.6}$$

the volume (bulk) viscosity

$$\eta_V = \frac{1}{Vk_BT}\int_0^\infty \langle (\varphi_{xx}(0) - \langle\varphi_{xx}\rangle)\,(\varphi_{xx}(t) - \langle\varphi_{xx}\rangle)\rangle\, dt; \tag{2.7}$$

the thermal conductivity

$$\lambda = \frac{1}{k_BT^2V}\int_0^\infty \langle Q_x(0)\, Q_x(t)\rangle\, dt, \tag{2.8}$$

where

$$\varphi_{xy} = \sum_i \frac{p_i^x p_i^y}{m_i} - \sum_{i>j}(x_i - x_j)\frac{\partial u_{ij}}{\partial y_j},$$

$$\varphi_{xx} = \sum_i \frac{(p_i^x)^2}{m_i} - \sum_{i>j}(x_i - x_j)\frac{\partial u_{ij}}{\partial x_j},$$

φ_{xy} and φ_{xx} are the components of the pressure tensor,

$$Q_x = \sum_i \frac{p_i^x p_i^s}{2m^2} + \sum_i \frac{p_i}{2m}\sum_{j\neq i} u_{ij} - \frac{1}{4}\sum_{i,j}\frac{1}{m}(p_i + p_j)\mathbf{r}_{ij}\frac{\partial u_{ij}}{\partial \mathbf{r}_i},$$

Q_x is the x component of the heat flux, and u_{ij} is the interparticle interaction potential.

The transport coefficients are currently being calculated by the MD method using Eqs. (2.5)–(2.8). However, there is a different calculation method, based on the Helfand formulas,[69,70] representing an analog of the Einstein relationship for the diffusion coefficient. For example, the viscosity can be defined as follows:

$$\eta t = \left\langle \left[\sum_i x_i(0)\, p_i^y(0) - \sum_i x_i(t)\, p_i^y(t)\right]^2\right\rangle. \tag{2.9}$$

We can easily see that in the theory of linear response and in the Helfand method the transport coefficients can be calculated by averaging a certain time-dependent function of the dynamic variables over an equilibrium ensemble, which can easily be done by the MD method using the ergodic hypothesis. A shortcoming of the Helfand method compared with the theory of linear response is the inability to find, by the Helfand method, the frequency dependences of the transport coefficients and the form of the correlation functions of the corresponding fluxes.

The temporal correlation functions of viscous fluxes of momentum and of the heat flux in a system of hard spheres were first found by the MD method by Alder *et al.*[15] and for a system of particles interacting in accordance with the Lennard-Jones potential by Lagar'kov and Sergeev,[4,26] and by Levesque *et al.*[50] Until then the time dependences of these functions were assumed to be exponential, in accordance with the relaxation theory. Naturally, stochastic-type equations, for example the Enskog equation[14] formulated for the calculation of the transport properties of very dense gases, also cannot be expected to yield any kind of time dependence of the temporal correlation functions other than exponential. However, at high densities when the dimensions of a particle become comparable with the mean free path, successive collisions are no longer independent. The existence of temporal correlations should result in a deviation from the exponential law of decay not only of the temporal velocity correlation function (TVCF) but also of other temporal correlation functions. Therefore, an analysis of temporal correlation functions carried out by the MD method makes it possible to determine correctly the range of validity of the stochastic-type transport equations and in the region where they are invalid, to obtain information which is as yet inaccessible by other methods.

An investigation of the temporal correlation function of the microscopic stress tensor of a system of hard spheres[15] demonstrated that for $V/V_0 > 2$ (V_0 is the volume in the close-packed case) the time dependence of the temporal correlation functions is approximately exponential. However, near the solidification curve the temporal correlation function of the nondiagonal component of the microscopic stress tensor has an extended positive "tail." Similar investigations in dense systems with realistic interaction potentials[4,26,50] also demonstrate that the positive tail of the temporal correlation function of the viscous flow of the momentum rises rapidly as the density is increased (Fig. 19). This is demonstrated particularly clearly in the case of densities and temperatures close to the triple point. The appearance of the tail is associated with collective effects. The MD experiments[50] indicate that these collective effects occur in a region of the order of the interparticle distances. The appearance of such effects can be readily understood if we bear in mind that the viscosity of a solid tends to infinity. In the liquid phase far from the solidification curve an intimation of this effect is seen. This is also observed in salt melts investigated by the MD method near the solidification line of the melt.[51]

The time dependence of the temporal correlation

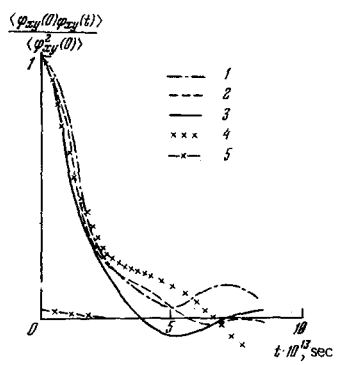

FIG. 19. Temporal correlation function for the viscous flow of momentum in argon: 1) $\rho = 1.16$ g/cm^3, $T = 120$°K; 2) $\rho = 1.31$ g/cm^3, $T = 127$°K; 3) $\rho = 1.37$ g/cm^3 $T = 100.2$°K; 4) $\rho = 1.41$ g/cm g/cm^3, $T = 84.5$°K; 5) kinetic part of the temporal correlation function of the momentum flux, $\rho = 1.16$ g/cm^3, $T = 120$°K.

function of the nondiagonal component of the microscopic stress tensor near the solidification curve can be described satisfactorily by the viscoelastic theory with two relaxation times. One of them is the usual relaxation time of the order of the time between two collisions, whereas the other is much greater and it is associated with the collective effects. In this connection we recall that shear waves are less damped near the solidification line and they appear at lower values of k compared with the model utilizing a single relaxation time (see Sec. 1.c).

It is worth noting the close relationship between the form of the TVCF and the temporal correlation function of the nondiagonal component of the microscopic stress tensor. As pointed out earlier, the TVCF and, particularly, its asymptotic behavior in time, can be derived by analyzing the hydrodynamic equations. A particle is then considered as a macroscopic object and the decay of its velocity is calculated on the basis of the Navier–Stokes equation with frequency-dependent transport coefficients. This approach to the calculation of the TVCF was first suggested by Zwanzig and Bixon.[71] If the generalized frequency-dependent viscosity is calculated using the theory with a single relaxation time, the extended negative plateau of this function—predicted by the MD calculations to occur near the triple point—is not observed. Allowance for a long positive tail of the temporal correlation function of the nondiagonal component of the stress tensor makes it possible to remove the resultant conflict and then the TVCF correlation function deduced by solving the Navier–Stokes equation is identical with the MD data for long times. Clearly, in the theory of thermal hydrodynamic fluctuations[23] the use of the viscoelastic model with two relaxation times would have also improved the agreement between the resultant TVCF and the MD data.

It is clear from the above discussion why the Stokes relationship $\eta Dd/T = \text{const}$ (where d is the diameter of a hard sphere) applied to a microscopic particle retains its validity over a wide range of densities.[15] The reduction in the diffusion coefficient at high densities because of a deeper negative minimum of the TVCF correlation function is compensated by an increase in the viscosity resulting from the extended positive tail of the temporal correlation function of the viscous flux of the momentum.[15] A more detailed discussion

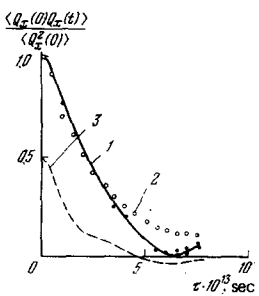

FIG. 20. Temporal correlation functions of the heat flux in argon[72] ($\rho = 1.41$ g/cm^3): 1) $T = 110$°K; 2) $T = 195$°K; 3) kinetic part of the temporal correlation function of the heat flux, $T = 110$°K.

of this topic in the two-dimensional case can be found elsewhere.[73]

The question of the relative contributions of the kinetic and potential parts of the momentum and heat fluxes to the integral of a temporal correlation function is very important in the theory of transport in liquids. Calculations of the kinetic contribution to the viscosity carried out for a system of particles with relativistic interaction potentials over a wide range of temperatures for transcritical densities[26,72] show that this contribution is very small: 2–5%. In the same range of thermodynamic parameters the contribution of the kinetic part of the heat flux to the thermal conductivity is considerably greater: of the order of 20–30% (Fig. 20). It is interesting to note that in the case of the kinetic part of the temporal correlation function of the microscopic stress tensor and heat flux and for the potential part of the heat flux the agreement between the hard-sphere calculations and those based on the Enskog theory remains good (to within 10%) right up to densities corresponding to $V/V_0 = 1.5$, whereas in the case of the potential part of the temporal correlation function of the microscopic stress theory the agreement is considerably poorer (the discrepancy is a factor of 1.5 for $V/V_0 = 1.6$ and a factor of 2 for $V/V_0 = 1.5$). These results demonstrate that the Enskog theory is unsuitable for the calculation of the viscosity of a dense system with $V/V_0 \lesssim 1.5$.

The first application of the MD method to the transport coefficients of liquids was the calculation of the diffusion coefficient of a system of hard spheres.[2] A calculation carried out using the formula in the theory of linear response and an application of the Einstein relationship $\langle \Delta r^2 \rangle = 6Dt$ demonstrate that the Enskog theory is satisfactory right up to a density of $\rho^* = 0.6$. Deviations between the Enskog theory and the MD calculations do not then exceed 20%. The results obtained suggest that at moderate densities and fairly high temperatures the Enskog theory gives satisfactory results for the other transport coefficients, as was indeed confirmed later.[15] The success of the Enskog theory in the description of the transport properties of a system of hard spheres, established by the MD method, has provided a simple means for computing the transport coefficients of liquids above the critical temperature[74]: a real liquid is considered as a system of hard spheres whose diameter is found from the thermodynamic properties and then the Enskog theory is used to find the transport coefficients. This calculation approach is characterized by a high precision (~10%) but it is still insufficiently self-consistent because it requires the knowledge of the temperature dependence of the sphere diameter. This dependence can only be obtained by numerical experiments.

The first calculation of the shear and volume viscosity and of the thermal conductivity of systems with realistic potentials was carried out by Bruin[76] using the Helfand formulas and by others[4,26,27,72] using the formulas of the linear response theory. However, it should be pointed out that a badly chosen range of the thermodynamic parameters prevented Bruin[76] from

providing a convincing comparison with the experimental data.

The simplest materials for checking the suitability of the MD method in calculation of the transport coefficients are liquefied rare gases, because the potentials of the interaction between particles in rare gases have been investigated more thoroughly than for other substances. However, even in the case of such a thoroughly studied material as liquid argon there are still considerable discrepancies between the published estimates of the "quality" of various potentials. We have mentioned earlier the successful application of the Lennard-Jones potential in the description of the thermodynamic properties of argon. Nevertheless, it is not *a priori* clear that this potential describes satisfactorily the transport properties.

A comparison[26] of the results of calculations carried out using three interaction potentials—the Lennard-Jones potential, the Buckingham potential,[77] and the potential deduced by Parson, Siska, and Lee[64] from the experiments on the scattering of argon atoms—demonstrated that the Lennard-Jones potential was the best. This comparison was carried out for self-diffusion coefficients, shear and bulk viscosities, and thermal conductivity over a wide range of temperatures but at a constant density of $\rho = 1.16$ g/cm^3. We compared[26] the results for the pure pair potential and the "effective" Lennard-Jones potential, which—as pointed out in Sec. 2.b—can be regarded as including many-particle effects. It follows from the results obtained that the interaction in a liquid is not identical with the interaction in the gaseous phase. The validity of using the Lennard-Jones potential in the calculating of the transport coefficients in liquid argon was confirmed by comparing the experimental data[34,79-83] with the calculations of the shear and volume viscosity and of the thermal conductivity carried out by the MD method over a wide range of temperatures and densities.[72,78]

The MD calculations[72] demonstrated that, at a fixed density, the shear viscosity is independent of temperature above the critical value and this is true right up to $T \sim 400$°K (Fig. 21). It should be pointed out that the experiments[81] carried out simultaneously and independently of the calculations[72] also demonstrated that the isochoric shear viscosity is independent of temperature at densities above the critical value. This confirmed once again Bachinski's view,[137] who drew attention to the constancy of the isochoric shear viscosity and suggested the formula $\eta = B/(\Omega - b)$ for this property; here, Ω is the specific volume, and B and b are constants governed by the properties of the liquid. The difference $\Omega - b$ represents the free volume of the liquid and the viscosity is inversely proportional to this free volume, which is practically independent of temperature if the density is fixed. Subsequently, Frenkel[131] justified the Bachinski formula from the point of view of the hole theory of liquids. It should also be pointed out that Frenkel's concept of the motion of particles in a liquid as occurring in accordance with the laws of macroscopic hydrodynamics also explains excellently the constancy of the isochoric shear viscosity. Applying Frenkel's relationship $\eta = k_B T/3\pi dD$ and the MD self-diffusion coefficient D, which give $D \propto \text{const} T/\rho^2$,[75] we obtain directly the temperature independence of the isochoric viscosity.

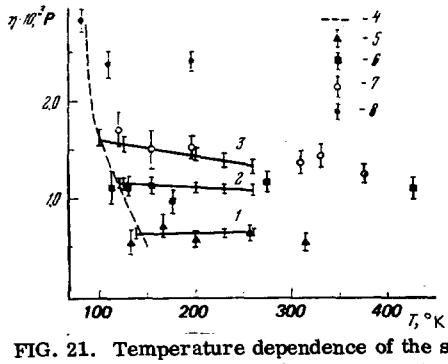

FIG. 21. Temperature dependence of the shear viscosity of argon plotted for various densities ρ (g/cm^3): 1) 0.9; 2) 1.16; 3) 1.31; 4) viscosity on saturation line; 5) 0.904; 6) 1.16; 7) 1.31; 8) 1.41. Symbols 1–3 represent experimental results[80] and symbols 5–8 represent calculated results.

The temperature dependence of the thermal conductivity at a fixed density obtained by the MD method[72] differs slightly from the experimental dependence and this is clearly due to the fact that the calculations[72] were carried out using a small number of particles in a cell, whereas an accurate calculation of the thermal conductivity requires consideration of a larger number of particles than in the cases of the shear and volume viscosity. An increase in the number of particles to 108 gives a better agreement[78] with experiment. On the whole, the results of Refs. 26, 72, and 78 are clear evidence of the great effectiveness of the formulas of the linear response theory in the calculation of the transport coefficients by the MD method. Attempts to calculate the transport coefficients of argon by the MD method[50,84] gave results not in good agreement with the experimental data. This is apparently due to the fact that in one case[50] the calculations were carried out at the triple point where, because of the high density, it is not possible to allow for the density dependences of the constants ε and σ in the Lennard-Jones potential. In the other case,[84] use was made of an incorrect method for the calculation of the temporal correlation function. When the method was modified,[78] the agreement with the experimental results and those reported elsewhere[72] was found to be good.

It is interesting to note that the MD calculations of the viscosity are in good agreement with the experimental results even when the number of particles in a cell is only $N = 32-36$.[26,72] A further increase in the number of particles to a few hundred[78] has little effect on the results. The situation is somewhat different in the case of the thermodynamic quantities. A precision of ~10% can be obtained by calculations for at least 100 particles in a cell. This is apparently due to the fact that the expression for the potential part of the pressure, which is being averaged, falls off as $1/r^6$, i.e., fairly slowly, whereas in the expressions for the temporal correlation function of the momentum flux

the averaged quantities that make the principal contributions fall off as $1/r^{12}$ and the interactions with distant particles may have little effect on the temporal correlation function of the momentum flux. Similar considerations explain why a calculation of the thermal conductivity of a small number of particles agrees less satisfactorily with the experimental data than a similar calculation of the viscosity. The point is that the expression for the temporal correlation function of the energy flux includes a term proportional to the interaction potential and, consequently, falling off as $1/r^6$. This term is found by multiplying the kinetic and potential parts of the energy flux vector, which occur in the correlation function $\langle Q_x(0)Q_x(t)\rangle$, and it is of the form $\Sigma_i p_i^2 p_i^x|_0 \Sigma_{i\neq k} u_{ik}(p_i^x+p_k^x)|_t$. For short times, i.e., in the range making the principal contribution to the integral of the temporal correlation function, this term is proportional to $T^2\bar{u}$ after the Gibbs averaging; here, $\bar{u}$ is the interaction energy per particle, which is a thermodynamic quantity and a large number of particles is required if calculations of it are to be accurate.

A very promising approach in investigations of the transport phenomena by the MD method is the creation of a deliberate lack of equilibrium in a cell. The main advantage of this method is the possibility of investigating nonlinear effects which appear under strongly inhomogeneous conditions.[85] The method of creating a deliberate lack of equilibrium has been used successfully in calculating the shear viscosity of argon. This gives the dependence of the shear viscosity on the stress tensor. In the case of low velocity gradients the results agree well with those obtained by us[26] and with the experimental data. Another very simple illustration of the possibility of creating a deliberate lack of equilibrium is the application of a static field to a cell filled with particles with opposite charges interacting in accordance with the Coulomb law. In this case the field dependence of the current across the wall of the cell gives directly the electrical conductivity. This scheme has not yet been implemented.

d) Calculation techniques and precision of the molecular dynamics method

In view of the fact that the MD calculations for systems composed of a few hundreds of particles are, at the present time, near the limit of capabilities of modern computers, the effectiveness of difference schemes becomes of basic importance. Calculation schemes for a system of hard spheres are relatively simple[2] and reduce to the solution of algebraic equations. The situation is more difficult in the case of systems with realistic potentials. This is due to the fact that at short distances the intermolecular interaction potential depends very strongly on the distance and in such cases the difference schemes suffer from poor convergence. Apparently this was the reason why an iteration scheme was used in the first calculations.[10] However, it was subsequently shown[59,4] that a very simple noniteration scheme, described by Eq. (I.1), ensures an entirely satisfactory precision. The criteria of the quality of a scheme are the degree to which the law of conservation of energy is obeyed and the dependence of the coordinate $\mathbf{r}(t)$ on the step in a difference scheme. A difference scheme is most conveniently tested on a one-dimensional problem. Calculations based on the scheme (I.1) and the Lennard-Jones potential demonstrated[4] that in 10^3 steps (corresponding to 2–3 oscillations in a potential well) the energy fluctuates within 2–3% and that the coordinate error for a step (in reduced units $t^*=ta\sqrt{\varepsilon/m}$) $\Delta t = 0.005$ in the same number of steps is ~3%.

It should be pointed out that ways of economizing the calculation time are not limited to selection of a good difference scheme. Other improvements are also possible. In considering a system with a large number of particles ($N \sim 10^3$) it is not necessary to calculate all the distances between the particles and all the interaction forces at each step. For particles at considerable distances ($\geq 3.3\sigma$) the Lennard-Jones potential is so small that it can be simply assumed to be zero. Over somewhat shorter distances in the range $2.5 < r < 3.3$ the interaction forces vary slowly with time and, therefore, they need not be calculated at every step of the difference scheme but every few steps. Implementation of such a scheme[59] reduced the calculation time by about an order of magnitude (the number of particles was $N = 864$). Correct selection of the calculation scheme made it possible to reduce the resultant error to a value considerably smaller than the error due to the use of periodic boundary conditions.

Frequent attempts have been made to estimate analytically the error resulting from the application of periodic boundary conditions. However, such estimates have been obtained only for the virial coefficients.[6-9] It has been found that the error in the second and third virial coefficients resulting from periodicity of the boundary conditions is of the order of $O(1/N)$. The dependence on the number of particles has also been estimated directly from the MD calculations by increasing this number to a few thousand. In the case of the diffusion coefficient of a system of hard spheres[16] this approach gives the result

$$D_N = D_\infty\left(1-\frac{2}{N}\right). \qquad (2.10)$$

The dependence is fairly weak and it shows that a system with 30–40 particles per cell gives results with the same precision as the experimental data.

The extrapolation method can be used to find accurate values of the quantities determined by the MD method and to eliminate the dependence on the boundary conditions. This is done by plotting $1/N$ along the x axis and the values of the investigated quantity $P_N(1/N)$ along the y axis. The set $P_N(1/N)$ is approximated by a linear function and the required value P is deduced as the value of this function at $1/N = 0$. This makes it possible to obtain reliable values of P even when only two points P_{N_1} and P_{N_2} are available.

Specific causes of the error appear in calculations of the transport coefficients by the MD method using the linear response theory. In the expressions for the transport coefficients (2.7)–(2.10) the temporal correlation function is integrated with respect to time from 0 to ∞. It is not realistic to carry out such integration

and, therefore, it is necessary to estimate the contribution of long times to the integral. This can be done using the hydrodynamic asymptotic behavior of the temporal correlation function discussed above. Estimates indicate that for $t > (3-5)\tau_0$, where τ_0 is the relaxation time, this contribution is small (~10%) and it decreases as the temperature is increased and the density is reduced. Extension of the integration time naturally reduces the error. Attempts have also been made[86] to estimate the error in the MD calculations of the temporal velocity correlation function $\langle v_i(0)v_i(t)\rangle$ due to the quantity $\langle v_i(\tau)v_i(t+\tau)\rangle$, being averaged in accordance with the ergodic hypothesis and the integration with respect to τ not being carried out up to ∞ but to some value T. If we assume that the velocity $v(t)$ is a Gaussian random quantity and introduce

$$\Delta(t) = \frac{1}{T}\int_0^T dS\,[v_i(s)v_i(s+t) - \langle v(s)v(s+t)\rangle], \tag{2.11}$$

then $\langle \Delta t\rangle = 0$, and the error due to the finite integration time can be found by calculating the second moment $\langle \Delta^2(t)\rangle$. If $v(t)$ is a Gaussian quantity, we can show that $\langle \Delta^2(t)\rangle \sim 2\tau_0/T$ and, consequently,

$$\frac{\langle v(0)v(t)\rangle_\infty}{\langle v^2\rangle_\infty} = \frac{\langle v(0)v(t)\rangle_T}{\langle v^2\rangle_\infty} \pm \sqrt{\frac{2\tau_0}{T}}. \tag{2.12}$$

Therefore, in calculating the temporal correlation function to within 2–3% (which corresponds to the experimental error) it is necessary to ensure that $T \sim 10^3\tau_0$. When additional averaging over the particles

$$\langle v_i(0)v_i(t)\rangle = \frac{1}{N}\sum_{i=1}^{N}\langle v_i(0)v_i(t)\rangle \tag{2.13}$$

is used, the error in Eq. (2.12) decreases as $1/\sqrt{N}$, which is easy to explain physically because averaging over the particles is equivalent to an increase in the averaging time in Eq. (2.12) by a factor of N. However, it should be pointed out that $v(t)$ is not really a Gaussian random quantity. Moreover, at the outset we have assumed that the temporal correlation function falls off exponentially at large values of t, which we know to be incorrect. All this makes it necessary to treat Eq. (2.12) with caution. Direct calculations demonstrate that the estimate given by Eq. (2.12) is somewhat too high.

In view of the above discussion we may conclude that the use of modern computers in calculation of the transport coefficients of classical systems by the MD method makes it possible to achieve in a reasonable time a precision comparable with that obtainable experimentally.

3. DYNAMICS OF A LIGHT CLASSICAL PARTICLE IN A DENSE MEDIUM OF DISORDERED HEAVY SCATTERERS

a) Formulation of the problem

The problem of the motion of a light particle among disordered scatterers arises in investigations of very many physical situations and its solution has direct applications to rarefied and dense gases, and to condensed media. The model for the limiting case of strongly rarefied scatterers is familiar under the name of the Lorentz gas model. The solution of the linearized Boltzmann equation, describing the behavior of a Lorentz gas, can be found in most textbooks on physical kinetics. However, the problem complicates greatly as soon as the scatterer density N increases. Even for a very simple type of interaction, such as that of a hard sphere of radius a with immobile point centers, the development of the kinetic theory for the $Na^3 \sim 1$ case involves fundamental difficulties. These difficulties appear because of the need to allow for the spatial and temporal correlations that occur when a particle moves in a dense medium, and they increase considerably in the case of "soft" interaction potentials.

As before, in the present section we shall consider all the problems from the point of view of nonequilibrium classical statistical mechanics, which naturally limits the range of validity of the results obtained. However, it should be remembered that the results of a self-consistent theory are extremely modest even in the case of a classical description. At present the theory[87] gives the first terms of the expansion, in terms of the density, of the reciprocal diffusion coefficient and predicts the existence of terms logarithmic in density. An investigation of the motion of a hard disk[126] among randomly distributed point scatterers, carried out by the MD method, has confirmed the existence of terms logarithmic in density in the case of a two-dimensional Lorentz gas. For a three-dimensional system the results of the MD calculations[88] of the motion of a hard sphere among point scatterers has demonstrated reasonable agreement with the theory in which the reciprocal diffusion coefficient is described by an expansion in powers of the density. However, at present it is hardly possible to identify the logarithmic terms for a three-dimensional case by the MD method and to demonstrate their existence because in this case the logarithmic terms play a less important role than in two-dimensional cases.

Apparently the most effective approach is the use of the MD method for investigating the motion of a light particle in a high-density disordered medium. At high scatterer densities basically new qualitative phenomena arise which do not occur in rarefied systems. They include, for example, a nonmonotonic energy dependence of the mobility, the appearance of percolation at negative particle energies, etc. (The percolation level is the minimum energy E_p of a classical particle in an arbitrary potential energy curve U for which there still exists a region in space with $E > U$ extending to infinity in all directions.) Even for the determination of such a relatively simple characteristic of the motion of a particle in a dense medium as the percolation level, it is necessary to use the Monte Carlo method specially developed for solving continuum problems.[138] More complex dynamic characteristics can be found reasonably consistently only by the MD method. Investigation of the phenomenon of percolation as such is hardly the purpose of the present section, especially as a recent review[139] has dealt with the problem of percolation and its relationship to the con-

ductivity of strongly inhomogeneous media. We shall consider the behavior of a particle in a disordered medium from a somewhat different angle, which has not yet been sufficiently thoroughly investigated, namely, we shall demonstrate a close relationship between the behavior of the TVCF and spatial correlation function of a particle (the latter representing its position relative to the scatterers), density of states, percolation level, and mobility; this relationship is revealed by calculations based on the exact microscopic approach. This approach has become possible because of the application of the MD method somewhat modified[91] to fit the specific nature of the problem under discussion. The value of the percolation level is found in this approach, together with many other macroscopic averages, and in determining this level the MD method is an important supplement of the Monte Carlo method.

Let a light particle to which we shall refer (because of subsequent applications) as an electron move in a field formed by scatterers:

$$U(r)=\sum_{j=1}^{N} u(\mathbf{R}_j-\mathbf{r}), \tag{3.1}$$

where $u(\mathbf{R}_j-\mathbf{r})$ is the electron–scatterer interaction potential; $\mathbf{r}$ is the coordinate of the electron; $\mathbf{R}_j$ is the coordinate of the scatterer.

If the asymptotic form of the interaction potential $u(r)$ at large distances is taken to be the polarization potential $\sim\alpha e^2/2r^4$, where α is the polarization constant, and some effective repulsion is assumed for short distances, the motion of a particle in the field (3.1) simulates a situation which occurs in a dense weakly ionized plasma of metal vapors at subscritical densities. In such a plasma subject to the conditions $\beta N_0\int u\,dr\gg 1$, $n^{1/3}e^2\beta<1$, where $\beta=1/k_BT$, n is the electron density, and N_0 is the density of neutral atoms, the interaction between an electron and neutral atoms predominates and the interaction of the electron with ions and with other electrons can be ignored. At such concentrations of heavy neutral particles an electron is always in the field of action of their forces and, naturally, is not free. These conditions occur not only in dense plasmas of metal vapors, but also in dense gases on injection into them of charged particles, for example, under the action of ionizing radiation, and also in many other physical systems.[140] All the subsequent results will be obtained for the electron–atom interaction potential of the form shown in Fig. 22, which simulates the interaction of an electron with a mercury atom. The selection of the potential describing the electron–atom interaction was discussed in detail by Lagar'kov and Sarychev.[92] It should be pointed out here that the main qualitative relationships, which will be demonstrated later, remain valid for any potential characterized by attraction over long distances and repulsion over short distances; for example, the ideas and method presented in this section can be applied to investigate the motion of a light ion or atom (for example, He^+ or He) moving in a very dense and heavy gas (for example, Xe).

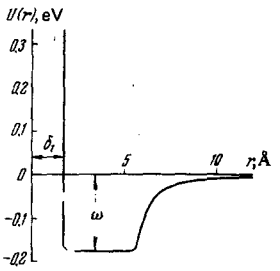

FIG. 22. Effective potential of the interaction between an electron and an Hg atom.

In this section we shall examine how the density of states, the electron–atom pair correlation function, and the TVCF of an electron moving in the field (3.1) vary with the electron energy and the density of the scattering atoms. We shall show that an investigation of these quantities by the MD method makes it possible to study the rapid rise of the conductivity from the value in a gas to a value close to that in a metal[89,95] as a result of a slight increase in the density at subcritical densities. In this way we shall use the MD method to describe the initial stage of a metal–insulator phase transition. Extension to supercritical densities is limited by the use of the classical ideas suitable for the description of the motion of an electron in a dense weakly ionized plasma. The criteria of the quasiclassical situation were given by Rice and Allnatt.[30]

Since in this problem the interaction of electrons with one another can be ignored, the conductivity of a system of electrons in the field (3.1) is given by the familiar expression[141]

$$\sigma_{xx}(\omega,\beta)=ne^2\beta Z^{-1}\int_{-\infty}^{+\infty} e^{-\beta E}\rho(E)\,D(E,\omega)\,dE, \tag{3.2}$$

where n is the electron density, $\rho(E)$ is the density of states,

$$Z=\int_{-\infty}^{+\infty} e^{-\beta E}\rho(E)\,dE, \tag{3.3}$$

$$D(E,\omega)=\int_{0}^{\infty}\cos\omega t\,\varphi_E(t)\,dt, \tag{3.4}$$

$\varphi_E(t)$ is the TVCF of an electron,

$$\varphi_E(t)=\langle v_x(0)v_x(t)\rangle_E, \tag{3.5}$$

v_x is the x-component of the electron velocity, and $\langle\,\rangle_E$ is the micorcanonical average over the initial momenta and coordinates of an electron for a fixed electron energy (the scatterer mass is assumed to be infinite), which is also averaged over all the possible scatterer configurations.

We shall now analyze the behavior of the quantities determining $\sigma_{xx}(\omega,\beta)$.

b) Density of states and spatial electron–atom correlation function

In the quasiclassical approximation the density of states is given by

$$\rho(E)=\frac{(2m)^{3/2}}{V\pi^2\hbar^3}\left\langle\!\!\left\langle\int\sqrt{E-U(\mathbf{r},\mathcal{R}_j)}\,d\mathbf{r}\right\rangle\!\!\right\rangle=\frac{m^3}{\pi^2\hbar^3}v_{av}, \tag{3.6}$$

where $v_{av}=1/V\langle\!\langle\int v(\mathbf{r},\mathcal{R}_j)d\mathbf{r}\rangle\!\rangle$, m is the electron mass, $v(\mathbf{r},\mathcal{R}_j)$ is the velocity of an electron at a point r in a scatterer configuration $\mathcal{R}_j$, and $\langle\!\langle\ \rangle\!\rangle$ denotes averaging

over the scatterer positions, which may be correlated with one another.

We can show[92] that the value of v_{av} can be calculated by the MD method from

$$\left\langle \int v(\mathbf{r}, \mathcal{R}_j)\, d\mathbf{r} \right\rangle = \lim_{T\to\infty} \frac{\left\langle \int_0^T v^4(t, \mathcal{R}_j)\, dt \right\rangle}{\left\langle \int_0^T v^3(t, \mathcal{R}_j)\, dt \right\rangle} V_g, \qquad (3.7)$$

where V_g is the volume accessible to classical motion.

The expression (3.7) can be interpreted on the basis of the following qualitative considerations.

The whole space in which the integration is carried out is divided into cubes of side $L_i = v_i \Delta t$, where $v_i = \sqrt{2[E - U(r_i)]}$, Δt is the integration step in the numerical solution of the equations of motion by the MD method, and v_i is the velocity of an electron at a point r_i. This division is possible because for $\Delta t \to 0$ the region of overlap of two cubes tends to zero faster than the volumes themselves. Then, the integral in Eq. (3.7) can be rewritten as the sum $\int v d\mathbf{r} = \Sigma_{i=1}^{M} v_i v_i^3 (\Delta t)^3$. Calculating now the integral $\int_0^T v_i^4 dt$ along a trajectory, we can traverse the whole volume. However, the contribution made to the integral by each of the points r_i is $v_i^4 \Delta t$, and in the limit $T \to \infty$ each such contribution is included many times. The degree of repetition can be allowed for by introducing a normalization factor $V_g / \Delta t^2 \int_0^T v^3 dt$, equal to the ratio of the accessible volume V_g to the total volume covered by the trajectory during its motion. The proportion of the accessible volume to the total can also be found by numerical methods.[92]

Figure 23 shows the energy dependence of the density of states calculated by the MD method for systems of correlated and uncorrelated scatterers. In allowing for the correlation between the scatterers it is assumed that they interact with one another as hard spheres of radius δ_1. Dimensionless units are used in Fig. 23 and some of the other figures. The energy is then measured in terms of the depth of the potential ε and the length in units of δ_1 (Fig. 22). The electron mass is taken to be unity. Then, the dimensionless time is

Figure 23 shows also the density of states in the Gaussian approximation, used widely in the theory of disordered systems. We can see that beginning from

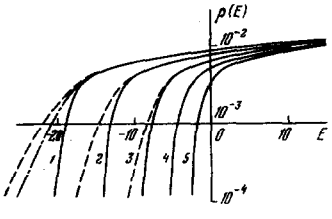

FIG. 23. Energy dependences of the density of electron states. The continuous curves represent correlated scatterers and the dashed curves the uncorrelated systems. 1) $N = 1.32 \times 10^{22}$ cm^{-3} ($N\delta_1^3 = 0.069$); 2) $N = 8.3 \times 10^{21}$ cm^{-3} ($N\delta_1^3 = 0.043$); 3) $N = 4.8 \times 10^{21}$ cm^{-3} ($N\delta_1^3 = 0.025$); 4) $N = 2.4 \times 10^{21}$ cm^{-3} ($N\delta_1^3 = 0.013$); 5) $N = 1.04 \times 10^{21}$ cm^{-3} ($N\delta_1^3 = 0.0054$). The chain curve represents the Gaussian approximation for case 1.

$E < u_{av} - \gamma$, where

$$u_{av} = 4\pi N_0 \int_{\delta_1}^{\infty} u(r) r^2 dr,$$

$$\gamma^2 = 2N_0 4\pi \int_{\delta_1}^{\infty} u^2 r^2 dr,$$

the Gaussian approximation overestimates the density of states. This is due to the fact that states of energies $E < u_{av} - \gamma$ belong to electrons localized at scatterer clusters. These clusters are created by an electron which attracts atoms and thus forms a cloud of higher density, and is then captured by the potential well of this cloud. The density of the scatterers in clusters is much higher than the average density of neutral atoms and, naturally, the Gaussian statistics is inapplicable to such large fluctuations of the density. The resultant clusters are similar in nature to those considered elsewhere[142] and the phenomenon itself is analogous to the localization of electrons by fluctuations of the impurity ion density in heavily doped semiconductors. The importance of clusters in the behavior of a dense plasma was first pointed out by Khrapak and Yakubov.[143] The structure of a cluster can be seen by considering the electron–atom spatial correlation function:

$$g(r, E) = \frac{1}{N 2\pi r^2 \Delta} \frac{1}{M} \sum_{k=1}^{M} \sum_{j} \frac{1}{T} \int_0^T \chi_\Delta(r - |\mathbf{r}(t, \mathcal{R}_k, E) - R_j|)\, dt, \qquad (3.8)$$

where $\chi_\Delta(x) = 1$ for $|x| \leq \Delta$, $\chi(x) = 0$ for $|x| > \Delta$, and $r(t, \mathcal{R}_k, E)$ is the trajectory of an electron in a scatterer configuration $\mathcal{R}_k$.

The quantity $g(r, E)$ is plotted in Fig. 24 for several values of the density and for an energy corresponding to a transition of an electron to a nonlocalized state, i.e., for values of the energy corresponding to the percolation level. Clearly, the percolation level decreases as the density increases. When the energy is increased, the function $g(r, E)$, calculated for the case of correlated scatterers, exhibits the first maximum and then a second one at lower energies. The existence of two maxima is due to the fact that the scatterers

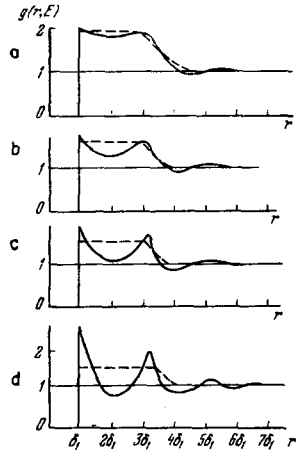

FIG. 24. Spatial electron—atom correlation function at energies equal to the percolation energy. The continuous curves represent correlated scatterers and the dashed curves an uncorrelated system. N(cm^{-3}): a) 1.32×10^{22}; b) 8.3×10^{21}; c) 2.4×10^{21}; d) 4.8×10^{21}.

interact with one another as hard spheres of radius δ_1. If the scatterers attracting an electron were close packed, the radius corresponding to the second maximum would have been equal to the radius of the second coordination sphere. Clearly, in the case of uncorrelated scatterers the quantity $g(r, E)$ should have one maximum which increases on reduction of the energy, as confirmed by the results in Fig. 24. Knowing the function $g(r, E)$, we can determine the average number of particles in a cluster N_{cl}. For $T \sim 1500°K$ and $N = 6 \times 10^{21}$ cm^{-3}, we have $N_{cl} \sim 20$, i.e., an electron is localized at a large cluster of scatterers which is characterized by a short-range order in the case of a correlated system. We can now understand the difference between the densities of states for the correlated and uncorrelated scatterers demonstrated in Fig. 23. The entropy of formation of a cluster is higher for completely disordered scatterer systems. If scatterers do not repel, a cluster assembles more readily and, therefore, a deep well forms in which an electron may have a large negative energy.

c) Temporal velocity autocorrelation function and constant-energy conductivity

As in Sec. 1, the TVCF of an electron moving in the field of the surrounding heavy scatterers can be found on the basis of the ergodic hypothesis

$$\varphi_E(t) = \lim_{M\to\infty} \frac{1}{M} \sum_{k=1}^{M} \lim_{T\to\infty} \frac{1}{T} \int_0^T v_x(t', \mathcal{R}_k)\, v_x(t'+t, \mathcal{R}_k)\, dt'. \qquad (3.9)$$

The results of calculations of $\varphi_E(t)$ for different energies and two densities are presented in Figs. 25 and 26. At high positive energies (an electron moves in a dense gas of heavy spheres and the attractive part is a weak perturbation) this correlation function is monotonically damped. However, at higher densities the behavior of the temporal velocity correlation function differs greatly from the exponential form even when the energy is high. As the energy is reduced, the function $\varphi_E(t)$ acquires a negative minimum, which reflects the oscillatory motion of an electron, i.e., an electron is localized for a time until it finds a passage in the potential barrier. Then, the integral $D(E, 0) = \int_0^\infty \varphi_E(t)dt$, representing the conductivity of electrons of a given energy E, differs considerably from zero: an electron can then escape to infinity along conducting channels. Finally, for a value of E such

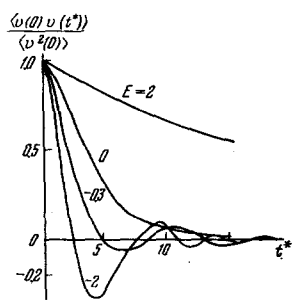

FIG. 25. Temporal velocity correlation function for motion in a field of correlated scatterers ($N = 1.04 \times 10^{21}$ cm^{-3}) plotted for different values of the energy against the relative time.

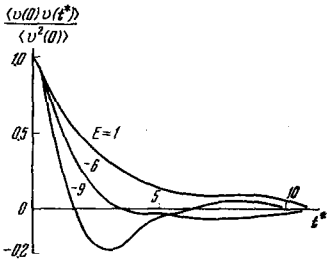

FIG. 26. Temporal velocity correlation function for motion in a field of correlated scatterers ($N = 4.8 \times 10^{21}$ cm^{-3}).

that $D(E, 0) = 0$, an electron becomes localized and makes no contribution to the conductivity. This definition of a localized electron agrees with that proposed by Mott.[140] Since the number of particles in a cluster is fairly large, the function $\varphi_E(t)$ is damped out rapidly also in the localized case because electron "forgets" its initial velocity on becoming entangled inside a cluster. Figure 27 gives the values of $D(E, 0)$ obtained for various densities. At all densities that have been investigated the value of $D(E, 0)$ rises by several orders of magnitude in a narrow range of energies. At lower densities the conductivity channels become open at higher energies. The maximum value of E at which $D(E, 0)$ is still zero determines the percolation level. Thus, an analysis of the TVCF enables us to investigate the phenomenon of percolation in the continuum model with a realistic interparticle interaction potential.

Since the fraction of the volume accessible to classical motion $C(E)$ is calculated as a function of the particle energy by finding the density of states while the percolation level can be deduced from the graphs of $D(E, 0)$, we can easily determine the dependence $C(E_p)$. This dependence $C(E_p)$ is plotted in Fig. 28 for the interparticle potential shown in Fig. 22. First of all, it is necessary to draw attention to the fact that the value of $C(E_p)$ depends strongly on the density of the system. At low densities, when the field correlation radius is small, $C(E_p)$ tends to the value of 0.32 obtained earlier.[93,138] The same value of $C(E_p)$ can also be found by an approach based on the use of a renormalized group.[94] However, at high densities of correlated scatterers the value of $C(E_p)$ decreases as the density is increased and is no longer universal. Variation of $C(E_p)$ over a wide range has been found also for non-Gaussian potentials.[138] In our opinion, this result is extremely important because it shows that, for real interaction potentials and a high density

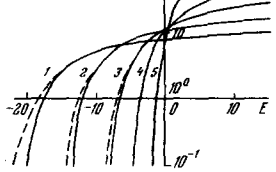

FIG. 27. Constant-energy conductivity $D(E, 0)$ plotted as a function of the energy for various densities. The notation is the same as in Fig. 23.

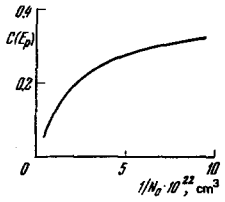

FIG. 28. Fraction of the critical volume plotted as a function of the density of atoms.

of correlated scatterers, it is not reasonable to expect universal relationships for determining the fraction of the accessible volume.

d) Calculation of the conductivity

The conductivity $\sigma(\beta, \omega)$ of a system can be calculated by determining the dependence of the total electron density (i.e., the density of electrons both in clusters and in the free state) on the density of the scattering atoms and on the temperature. Clearly, this can be done by finding the free energy of the system and minimizing it. The dependence of the electron density on the density of neutral atoms can be understood qualitatively on the basis of a simple model in which electrons and ions interact identically with atoms and atoms do not interact with one another (this calculation is included in the rigorous calculations by the MD method[92]). Then, the expression for the free energy becomes[143]

$$F = F_0 - 2TVnN_0 \int dr e^{-\beta u(r)} - 1, \tag{3.10}$$

where F_0 is the free energy of an ideal plasma; hence, we obtain directly the ionization equilibrium equation

$$n^2 = \lambda_T^{-3} N_0 \exp\left[-E_i\beta + 2N_0 \int dr\,(e^{-\beta u} - 1)\right], \tag{3.11}$$

where λ_T is the thermal wavelength of an electron and E_i is the ionization energy of a neutral atom.

Equation (3.11) differs from the Saha equation by the appearance of a positive term in the argument of the exponential function and this term increases as the degree of departure of the system from the ideal case increases. Consequently, the electron density begins to rise rapidly on attainment of fairly high densities and this explains partly the steep rise of the conductivity $\sigma(\beta, 0)$ in a narrow range of densities. Using the values of $\rho(E)$, $D(E, \omega)$, and n calculated by the MD method, we can find the conductivity $\sigma(\omega, \beta)$ and explain the observed rise of the static conductivity $\sigma(0, \beta)$ during the first stage of plasma metallization. The data found by the MD method[92,144] are in good agreement with the experimental results in the subcritical range at all temperatures for which such data are available (Fig. 29). The use of the MD method for a calculation of $\sigma(\omega, \beta)$ makes it possible to predict qualitatively the change in the free–free absorption of visible infrared radiation by electrons at high plasma densities. The expected anomalies are associated with a change in the form of the TVCF on localization of an electron in a cluster of atoms.

We shall conclude this section by noting that the MD method has been found to be exceptionally effective in the calculation of the thermo-emf of a dense mercury plasma.

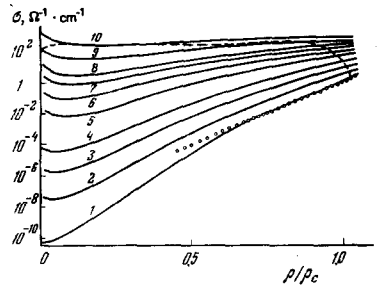

FIG. 29. Dependence of the conductivity of a mercury plasma on the relative density (ρ_c is the critical density of Hg). The circles represent the experimental results[145] obtained at $T = 1850$°K. The continuous curves are calculated tof T(°K): 1) 1823; 2) 2200; 3) 2600; 4) 3000; 5) 4000; 6) 5000; 7) 6000; 8) 7000; 9) 10 000; 10) 15 000. The dashed curve is the boundary of the electron density lower than $0.1N$.

CONCLUSIONS

The number of papers utilizing the MD method is increasing in an avalanche-like manner. The branches of physics in which the MD method has been used successfully are frequently so far apart that a separate review could be written for many of these applications. Moreover, there is a certain number of papers which describe new applications and are interesting *per se* but yet do not give the complete physical picture of the nature of motion in dense systems characterized by a fairly complex interaction law. For this reason we have confined the present review to a detailed analysis of systems with relatively simple interaction potentials, especially as only such systems give us hope to expect soon the development of physical ideas based on the MD method in the same way as on the experimental data.

Readers interested in the MD results obtained in investigations of diatomic liquids with spherically asymmetric interaction potentials can find them in the review by Berne and Harp[96] and also elsewhere.[97,98] Molecular dynamics investigations have also been made of mixtures of simple liquids,[99-105,115] melts of salts,[38,42,106,107] liquid metals,[108,109,150,151] scattering of light in liquids and melts,[110-114] relaxation of dipole polarization,[113] thermodynamic and transport properties of water,[116-119] dense strongly ionized plasmas,[120,152,153] structure and properties of microclusters,[127,128,154-158] and formation of dimers.[129,130]

The MD method has been applied to nonergodic systems[121-124] and to the formation of cluster waves in solids.[125] We can thus see that the potentialities of the MD method are extremely wide and the range of its applications is growing continuously. In particular, there are grounds for expecting that attempts to study quantum systems will be made in the nearest future.

[1]Fizika prostykh zhidkostei (Collection: Physics of Simple Liquids, Russ. Transl.), Mir, M., 1971.

[2]B. J. Alder and T. Wainwright, in: Proc. Intern. Symposium on Transport Processes in Statistical Mechanics, Brussels, 1956 (ed. by I. Prigogine), Interscience, New York, 1958, p. 97.
[3]N. T. Kovalenko and I. Z. Fisher, Usp. Fiz. Nauk **108**, 209 (1972) [Sov. Phys. Usp. **15**, 592 (1973)].
[4]A. N. Lagar'kov and V. M. Sergeev, Teplofiz. Vys. Temp. **8**, 1309 (1970).
[5]I. Z. Fisher, Statisticheskaya teoriya zhidkosti (Statistical Theory of Liquids), Fitzmatgiz, M., 1961.
[6]I. Oppenheim and P. Mazur, Physica (Utrecht) **23**, 197 (1957).
[7]J. L. Lebowitz and J. K. Percus, Phys. Rev. **122**, 1675 (1961).
[8]I. Z. Fisher, Dokl. Akad. Nauk B. SSR **4**, 148 (1960).
[9]J. E. Mayer, J. Phys. Chem. **66**, 591 (1962).
[10]A. Rahman, Phys. Rev. **136**, A405 (1964).
[11]J. O. Hirschfelder, C. F. Curtiss, and R. B. Bird, Molecular Theory of Gases and Liquids, Wiley, New York, 1954, p. 624.
[12]B. J. Alder and T. Einwohner, J. Chem. Phys. **43**, 3399 (1965).
[13]T. Einwohner and B. J. Alder, J. Chem. Phys. **49**, 1458 (1968).
[14]D. Enskog, K. Sven. Vetenskapsakad. Handl. **63**, No. 4 (1922).
[15]B. J. Alder, D. M. Gass, and T. E. Wainwright, J. Chem. Phys. **53**, 3813 (1970).
[16]B. J. Alder and T. E. Wainwright, Phys. Rev. Lett. **18**, 988 (1967).
[17]B. J. Alder and T. E. Wainwright, Phys. Rev. A **1**, 18, (1970).
[18]Y. Pomeau, J. Chem. Phys. **57**, 2800 (1972).
[19]D. Levesque and W. T. Ashurst, Phys. Rev. Lett. **33**, 277 (1974).
[20]M. H. Ernst, E. H. Hauge, and J. M. J. van Leeuwen, Phys. Lett. A **34**, 419 (1971).
[21]M. H. Ernst, E. H. Hauge, and J. M. J. van Leeuwen, Phys. Rev. A **4**, 2055 (1971).
[22]R. Zwanzig and M. Bixon, Phys. Rev. A **2**, 2005 (1970).
[23]I. Z. Fisher, Zh. Eksp. Teor. Fiz. **61**, 1647 (1971) [Sov. Phys. JETP **34**, 878 (1972)].
[24]P. L. Fehder, J. Chem. Phys. **50**, 2617 (1969).
[25]G. W. Robinson, Mol. Phys. **3**, 301 (1960).
[26]A. N. Lagar'kov and V. M. Sergeev, Teplofiz. Vys. Temp. **11**, 513 (1973).
[27]D. Levesque and L. Verlet, Phys. Rev. A **2**, 2514 (1970).
[28]M. S. Wertheim, Phys. Rev. Lett. **10**
[29]E. J. Thiele, J. Chem. Phys. **38**, 1959 (1963); Y. Hiwartari, H. Matsuda, T. Ogawa, N. Ogita, and A. Ueda, Prog. Theor. Phys. **52**, 1105 (1974).
[30]S. A. Rice and A. R. Allnatt, J. Chem. Phys. **34**, 2144 (1961).
[31]A. R. Allnatt and S. A. Rice, J. Chem. Phys. **34**, 2156 (1961).
[32]P. Gray and S. A. Rice, J. Chem. Phys. **41**, 3689 (1964).
[33]B. A. Lowry, S. A. Rice, and P. Gray, J. Chem. Phys. **40**, 3673 (1964).
[34]L. D. Ikenberry and S. A. Rice, J. Chem. Phys. **39**, 1561 (1963).
[35]A. N. Lagar'kov and V. M. Sergeev, Teplofiz. Vys. Temp. **13**, 438 (1975).
[36]E. Helfand, Phys. Rev. **119**, 1 (1960).
[37]J. Ross, J. Chem. Phys. **24**, 375 (1956).
[38]V. M. Sergeev, Avtoreferat kand. dissertatsii (Author's Abstract of Thesis for Candidate's Degree), Institute of High Temperatures, Academy of Sciences of the USSR, M., 1973.
[39]S. A. Rice, Trans. Faraday Soc. **58**, 499 (1962).
[40]B. Berne and S. A. Rice, J. Chem. Phys. **40**, 1347 (1964).
[41]A. Rahman, J. Chem. Phys. **45**, 2585 (1966).
[42]S. I. Smedley and L. V. Woodcock, J. Chem. Soc. Faraday Trans. II, **70**, 955 (1974).
[43]A. F. Collings and L. A. Woolf, Aust. J. Chem. **24**, 225 (1971).
[44]L. Van Hove, Phys. Rev. **95**, 249 (1954).
[45]L. Van Hove, Physica (Utrecht) **24**, 404 (1958).
[46]B. R. A. Nijboer and A. Rahman, Physica (Utrecht) **32**, 415 (1966).
[47]C. H. Chung and S. Yip, Phys. Rev. **182**, 323 (1969).
[48]R. C. Desai and M. Nelkin, Phys. Rev. Lett. **16**, 839 (1966).
[49]A. Rahman, Phys. Rev. Lett. **19**, 420 (1967).
[50]D. Levesque, L. Verlet, and J. Kurkijarvi, Phys. Rev. A **7**, 1690 (1973).
[51]A. Rahman, in: Neutron Inelastic Scattering (Proc. Fourth Intern. Symposium, Copenhagen, 1968), Vol. 1, International Atomic Energy Agency, Vienna, 1968, p. 561.
[52]W. G. Hoover and B. J. Alder, J. Chem. Phys. **46**, 686 (1967).
[53]J. G. Kirkwood, E. K. Maun, and B. J. Alder, J. Chem. Phys. **18**, 1040 (1950).
[54]D. Levesque, Physica (Utrecht) **32**, 1985 (1966).
[55]B. J. Alder and T. E. Wainwright, J. Chem. Phys. **31**, 459 (1959).
[56]B. J. Alder and T. E. Wainwright, J. Chem. Phys. **33**, 1439 (1960).
[57]B. J. Alder and T. E. Wainwright, Phys. Rev. **127**, 359 (1962).
[58]W. G. Hoover and B. J. Alder, J. Chem. Phys. **46**, 686 (1967).
[59]L. Verlet, Phys. Rev. **159**, 98 (1967).
[60]A. van Itterbeek, O. Verbeke, and K. Staes, Physica (Utrecht) **29**, 742 (1963).
[61]A. Michels, H. Wijker, and Hk. Wijker, Physica (Utrecht) **15**, 627 (1949).
[62]R. D. Present, Contemp. Phys. **12**, 595 (1971).
[63]J. H. Dymond and B. J. Alder, J. Chem. Phys. **54**, 3472 (1971).
[64]J. M. Parson, P. E. Siska, and Y. T. Lee, J. Chem. Phys. **56**, 1511 (1972).
[65]M. Klein and H. J. M. Hanley, J. Chem. Phys. **53**, 4722 (1970).
[66]V. M. Jansoone and O. B. Verbeke, Ber. Bunsenges. Phys. Chem. **76**, 157 (1972).
[67]L. Verlet, Phys. Rev. **165**, 201 (1968).
[68]B. J. Alder, Phys. Rev. Lett. **12**, 317 (1964).
[69]E. Helfand, Phys. Rev. **119**, 1 (1960).
[70]R. Zwanzig, Annu. Rev. Phys. Chem. **16**, 67 (1965).
[71]R. Zwanzig and M. Bixon, Phys. Rev. A **2**, 2005 (1970).
[72]A. N. Lagar'kov and V. M. Sergeev, Teplofiz. Vys. Temp. **11**, 1162 (1973).
[73]T. E. Wainwright, B. J. Alder, and D. M. Gass, Phys. Rev. A **4**, 233 (1971).
[74]J. H. Dymond and B. J. Alder, J. Chem. Phys. **45**, 2061 (1966).
[75]J. J. van Loef, Phys. Lett. A **35**, 169 (1971).
[76]C. Bruin, Phys. Lett. A **28**, 777 (1969).
[77]M. J. Ross and B. J. Alder, J. Chem. Phys. **46**, 4203 (1967).
[78]A. K. Ashurov, A. M. Evseev, and A. A. Adkhamov, Dokl. Akad. Nauk SSSR **220**, 396 (1975).
[79]B. A. Lowry, S. A. Rice, and P. Gray, J. Chem. Phys. **40**, 3673 (1964).
[80]N. F. Zhdanova, Zh. Eksp. Teor. Fiz. **31**, 724 (1956) [Sov. Phys. JETP **4**, 749 (1957)].
[81]V. P. Slyusar', N. S. Rudenko, and V. M. Tret'yakov, Teplofizicheskie svoĭstva veshchestv i materialov (Termophysical Properties of Substances and Materials), No. 7, Izd. Standartov, M., 1973.
[82]D. G. Naugle, J. H. Lunsford, and J. R. Singer, J. Chem. Phys. **45**, 4469 (1966).
[83]W. M. Madigosky, J. Chem. Phys. **46**, 4441 (1967).
[84]A. M. Evseev and A. N. Shinkarev, Zh. Fiz. Khim. **46**, 1452 (1972).
[85]W. T. Ashurst and W. G. Hoover, Phys. Rev. Lett. **31**, 206 (1973).
[86]R. Zwanzig and N. K. Ailawadi, Phys. Rev. **182**, 280 (1969).
[87]A. Weijland and J. M. J. van Leeuwen, Physica (Utrecht) **38**, 35 (1968).
[88]C. Bruin, Physica (Utrecht) **72**, 261 (1974).

[89]V. A. Alekseev and A. A. Vecenov, Usp. Fiz. Nauk **102**, 665 (1970) [Sov. Phys. Usp. **13**, 830 (1971)].
[90]A. G. Khrapak and I. T. Yakubov, Teplofiz. Vys. Temp. **9**, 1139 (1971).
[91]A. N. Lagar'kov and A. K. Sarychev, Zh. Eksp. Teor. Fiz. **68**, 641 (1975) [Sov. Phys. JETP **41**, 317 (1975)].
[92]A. N. Lagar'kov and A. K. Sarychev, Teplofiz. Vys. Temp. **15**, 645 (1977).
[93]S. Kirkpatrick, Phys. Rev. Lett. **36**, 69 (1976).
[94]A. K. Sarychev, Zh. Eksp. Teor. Fiz. **72**, 1001 (1977) [Sov. Phys. JETP **45**, 524 (1977)].
[95]I. K. Kikoin and A. P. Senchenkov, Fiz. Met. Metalloved. **24**, 843 (1967).
[96]B. J. Berne and G. D. Harp, Adv. Chem. Phys. **17**, 63 (1970).
[97]J. Barojas, D. Levesque, and B. Quentrec, Phys. Rev. A **7**, 1092 (1973).
[98]P. S. Y. Cheung and J. G. Powles, Mol. Phys. **30**, 921 (1975).
[99]B. Borstnik and A. Azman, Chem. Phys. Lett. **11**, 374 (1971).
[100]B. Borstnik and A. Azman, Ber. Bunsenges. Phys. Chem. **75**, 392 (1971).
[101]B. J. Alder, J. Chem. Phys. **40**, 2742 (1964).
[102]K. C. Mo, K. E. Gubbins, G. Jacucci, and I. R. McDonald, Mol. Phys. **27**, 1173 (1974).
[103]B. J. Alder, W. E. Allsy, and J. H. Dymond, J. Chem. Phys. **61**, 1415 (1974).
[104]V. M. Sergeev, Zh. Fiz. Khim. **50**, 2624 (1976).
[105]A. M. Evseev and A. V. Chelovskiĭ, Vestn. Mosk. Univ. Khim. **26**, 279 (1971).
[106]F. Lantelme, P. Turq, B. Quentrec, and J. W. E. Lewis, Mol. Phys. **28**, 1537 (1974).
[107]L. Woodcock, Chem. Phys. Lett. **10**, 257 (1971).
[108]A. Paskin and A. Rahman, Phys. Rev. Lett. **16**, 300 (1966).
[109]A. Paskin, Adv. Phys. **16**, 223 (1967).
[110]J. H. R. Clarke, S. Miller, and L. V. Woodcock, in: Molecular Motions in Liquids (Proc. Twenty-Fourth Annual Meeting of Societe de Chimie Physique, Paris-Orsay, 1972), ed. by J. Lascombe, publ. by Reidel, Dordrecht, Holland and Boston, 1974, p. 495.
[111]J. H. R. Clarke and L. V. Woodcock, J. Chem. Phys. **57**, 1006 (1972).
[112]L. V. Woodcock, Chem. Phys. Lett. **10**, 257 (1971).
[113]B. J. Alder, J. J. Weis, and H. L. Strauss, Phys. Rev. A **7**, 281 (1973).
[114]B. J. Alder, H. L. Strauss, and J. J. Weis, J. Chem. Phys. **59**, 1002 (1973).
[115]A. M. Evseev, M. I. Shakhparonov, and G. P. Misyurina, Zh. Fiz. Khim. **44**, 2999 (1970).
[116]A. Rahman and F. H. Stillinger, J. Chem. Phys. **55**, 3336 (1971).
[117]A. Rahman and F. H. Stillinger, in: Molecular Motions in Liquids (Proc. Twenty-Fourth Annual Meeting of Societe de Chimie Physique, Paris-Orsay, 1972), ed. by J. Lascombe, publ. by Reidel, Dordrecht, Holland and Boston, 1974, p. 479.
[118]F. H. Stillinger and A. Rahman, J. Chem. Phys. **61**, 4973 (1974).
[119]F. H. Stillinger and A. Rahman, J. Chem. Phys. **60**, 1545 (1974).
[120]G. E. Norman and A. A. Valuev, in: Proc. Twelfth Inter. Conf. on Phenomena in Ionized Gases, Eindhoven, 1975, p. 257.
[121]W. G. Rudd and H. L. Frisch, J. Comput. Phys. **7**, 394 (1971).
[122]C. Carlier and H. L. Frisch, Phys. Rev. A **7**, 348 (1973).
[123]H. H. Szu, J. Bdzil, C. Carlier, and H. L. Frisch, Phys. Rev. A **9**, 1359 (1974).
[124]N. Saito, N. Ooyama, Y. Aizawa, and H. Hirooka, Progr. Theor. Phys. Suppl. No. 45, 209 (1970).
[125]T. Schneider and E. Stoll, Phys. Rev. Lett. **35**, 296 (1975).
[126]C. Bruin, Phys. Rev. Lett. **29**, 1670 (1972).
[127]C. L. Briant and J. J. Burton, J. Chem. Phys. **63**, 2045 (1975).
[128]C. L. Briant and J. J. Burton, J. Chem. Phys. **63**, 3327 (1975).
[129]H. W. Harrison and W. C. Schieve, J. Chem. Phys. **58**, 3634 (1973).
[130]W. C. Schieve and H. W. Harrison, J. Chem. Phys. **61**, 700 (1974).
[131]Ya. I. Frenkel' (J. Frenkel), Kineticheskaya teoriya zhidkosteĭ, Izd. AN SSSR, M., 1945 (Kinetic Theory of Liquids, Oxford University Press, Oxford, 1946, reprinted by Dover, New York, 1954).
[132]P. A. Egelstaff, Adv. Phys. **11**, 203 (1962).
[133]K. Skold, J. M. Rowe, G. Ostrowski, and P. D. Randolph, "Neutron Inelastic Scattering Study of Liquid Argon," Report No. AE-445, Ab. Atomenergi, Stockholm, Sweden, 1972.
[134]L. Verlet, in: Molecular Motions in Liquids (Proc. Twenty-Fourth Annual Meeting of Societe de Chimie Physique, Paris-Orsay, 1972), ed. by J. Lascombe, publ. by Reidel, Dordrecht, Holland and Boston, 1974, p. 469.
[135]J. M. Ziman, Principles of the Theory of Solids, Cambridge University Press, Cambridge, 1964 (Russ. Transl., Mir, M., 1966).
[136]J. G. Kirkwood, J. Chem. Phys. **14**, 180 (1946).
[137]A. I. Bachinski, Z. Phys. Chem. (Leipzig) **84**, 643 (1913).
[138]A. S. Skal, B. I. Shklovskiĭ, and A. L. Éfros, Pis'ma Zh. Eksp. Teor. Fiz. **17**, 522 (1973) [JETP Lett. **17**, 377 (1973)].
[139]V. I. Shklovskiĭ and A. L. Éfros, Usp. Fiz. Nauk **117**, 401 (1975) [Sov. Phys. Usp. **18**, 845 (1975)].
[140]N. F. Mott, "Electrons in disordered structures," Adv. Phys. **16**, 49 (1967) (Russ. Transl., Mir, M., 1969).
[141]R. Kubo, H. Hasegawa, and N. Hashitsume, J. Phys. Soc. Jpn. **14**, 56 (1959).
[142]I. M. Lifshits and S. A. Gredeskul, Zh. Eksp. Teor. Fiz. **57**, 2209 (1969) [Sov. Phys. JETP **30**, 1197 (1970)].
[143]A. G. Khrapak and I. T. Yakubov, Zh. Eksp. Teor. Fiz. **59**, 945 (1970) [Sov. Phys. JETP **32**, 514 (1971)].
[144]A. N. Lagar'kov and A. K. Sarychev, Teplofiz. Vys. Temp. **15**, 645 (1977).
[145]F. Hensel and E. U. Franck, Rev. Mod. Phys. **40**, 697 (1968).
[146]A. Rahman, Phys. Rev. Lett. **12**, 575 (1964).
[147]M. Tanaka and Y. Fukui, Prog. Theor. Phys. **53**, 1547 (1975).
[148]B. Borstnik and A. Azman, Chem. Phys. Lett. **12**, 620 (1972).
[149]V. G. Baĭdakov, A. E. Galashev, and V. P. Skripov, Fiz. Nizk. Temp. **2**, 957 (1976) [Sov. J. Low Temp. Phys. **2**, 469 (1976)].
[150]V. A. Polukhin, M. M. Dzugutov, A. M. Evseev, B. R. Gel'chinskiĭ, V. F. Ukhov, N. A. Vatolin, and O. A. Esin, Dokl. Akad. Nauk SSSR **223**, 650 (1975).
[151]N. A. Vatolin, I. T. Sryvalin, A. M. Evseev, V. A. Polukhin, B. R. Gel'chinskiĭ, V. F. Ukhov, and O. A. Esin, Dokl. Akad. Nauk SSSR **219**, 1394 (1974).
[152]A. A. Valuev and G. É. Norman, Teplofiz. Vys. Temp. **15**, 689 (1977).
[153]A. A. Valuev and G. É. Norman, Teplofiz. Vys. Temp. **15**, 191 (1977).
[154]A. A. Insepov and G. É. Norman, Zh. Eksp. Teor. Fiz. **73**, 1517 (1977) [Sov. Phys. JETP **46**,798 (1977)].
[155]D. J. McGinty, J. Chem. Phys. **55**, 580 (1971).
[156]D. J. McGinty, J. Chem. Phys. **58**, 4733 (1973).
[157]W. D. Kristensen, E. J. Jensen, R. M. J. Cotterill, J. Chem. Phys. **60**, 4161 (1974).
[158]S. P. Protsenko and V. P. Skripov, Fiz. Nizk. Temp. **3**, 5 (1977) [Sov. J. Low Temp. Phys. **3**, 1 (1977)].

Translated by A. Tybulewicz